Doctoral Thesis

Mechanisms of interaction between auxin and

brassinosteroid pathways in *Arabidopsis thaliana*

Taisuke Nagase

2015

Contents

Abstract

Auxin modulates plant tropic responses to light and gravity. Auxin is also involved in such diverse processes as division, elongation and differentiation of plant cells, organ patterning, vascular development etc. To understand the molecular mechanism of auxin-mediated root elongation, we carried out screening to isolate auxin-hypersensitive (*axhs*) mutants of *Arabidopsis thaliana*. The T-DNA insertional mutant *axhs1* was selected on the basis of root phenotypes associated with auxin sensitivity. Results from brassinosteroid (BR) feeding experiments, TAIL-PCR and genetic analyses indicate that *AXHS1* encodes DWF4, which catalyzes the rate limiting step of BR biosynthesis. The *axhs1* mutant shows increased sensitivity to indole-3-acetic acid (IAA), the synthetic auxin 2,4-dichlorophenoxyacetic acid (2,4-D), auxin transport inhibitors such as 2,3,5-triiodobenzoic acid (TIBA) and *N*-1-naphthylphthalamic acid (NPA), and the antiauxin *p*-chlorophenoxyisobutyric acid (PCIB) for the root elongation response. Analysis of the expression of the *DR5:GUS* and *HS:AXR3NT-GUS* reporter genes in wild type and *axhs1* genotypes, and characterization of double mutants between *axhs1* and mutants affected in auxin biosynthesis (*wei2-1*), auxin transport (*aux1-7, eir1-1*) and auxin signal transduction (*tir1-1, axr1-3, axr2-1*) indicate that auxin hypersensitivity in *axhs1* is mediated by the auxin-signaling pathway and an AUX1, EIR1/PIN2 dependent auxin uptake. We propose a model in which the ratio of the endogenous auxin-to-BR concentration controls auxin signal transduction by modulation of auxin transport and stability of AUX/IAA repressor proteins.

Abbreviations

ACC	1-amino-cyclopropane-1-carboxylic acid
ABC	ATP-binding cassette
ABRC	*Arabidopsis* biological research center
AFB	auxin signaling F-box protein
ARF	auxin response factor
ASA	alpha subunit of anthranilate synthase
ASK	*Arabidopsis* serine/threonine kinase
AXHS	auxin-hypersensitive
AXR	auxin-resistant
AUX/IAA	auxin/indole-3-acetic acid
AuxRE	auxin response element
BES	*bri1*-EMS (ethyl methanesulfonate-mutagenized)-suppressor
BIN	brassinosteroid-insensitive
BL	brassinolide
bp	base pair
BR	brassinosteroid
BRI	brassinosteroid-insensitive
Brz	brassinazole
BZR	brassinazole-resistant
CAPS	cleaved amplified polymorphic sequence
CUL	cullin
Col	Columbia
DET	de-etiolated
DWF	dwarf
DIM	diminuto (diminutive)
EIR	ethylene insensitive root
GUS	β-glucuronidase

HS	heat shock
IAA	indole-3-acetic acid
IPA	indole-3-pyruvic acid
NAA	1-naphthaleneacetic acid
NPA	*N*-1-naphthylphthalamic acid
NPH	non-phototropic hypocotyl
PAT	polar auxin transport
PCIB	*p*-chlorophenoxyisobutyric acid
PCR	polymerase chain reaction
PIN	pin-formed
RT-PCR	reverse transcription- polymerase chain reaction
SAUR	small auxin-upregulated RNA
SCF	serine/threonine kinase-cullin-F-box protein complex
SD	standard deviation
SUR	superroot
TAA	tryptophan amino transferase of *Arabidopsis*
TAIL-PCR	thermal asymmetric interlaced- polymerase chain reaction
TIBA	2,3,5-triiodobenzoic acid
TIR	transport inhibitor response
WT	wild type
WEI	weak ethylene insensitive
X-Gluc	5-bromo-4-chloro-3-indolyl-β-D-glucuronide
2,4-D	2,4-dichlorophenoxyacetic acid

Introduction

The plant hormone auxin, typified by indole-3-acetic acid (IAA), has been implicated in the regulation of plant growth and developmental processes such as cell division and expansion, lateral root formation, apical dominance, phototropism and gravitropism (Woodward and Bartel 2005).

Biochemical and molecular genetics approaches, including the isolation and characterization of *Arabidopsis* mutants and the cloning of the corresponding genes, have been a valuable strategy for the elucidation of auxin biosynthesis, transport and signal transduction pathways. Most of the mutants isolated so far have been selected on the basis of root phenotypes associated with auxin and/or auxin transport inhibitors resistance. Many of those mutants display cross-resistance to hormones such as ethylene, cytokinin, or abscisic acid. These pleotropic phenotypes illustrate the existence of cross-talk between different hormone signaling pathways (Woodward and Bartel 2005; Lau et al. 2008).

The auxin-deficient mutant *wei2.1* is a loss-of-function mutant of the *ASA1* gene, which encodes the α-subunit of a rate limiting enzyme of tryptophan biosynthesis, anthranilate synthase (Stepanova et al. 2005). Tryptophan has been shown to be the main precursor for IAA in plants (Woodward and Bartel 2005, Mashiguchi et al. 2011). Mutant analyses have clearly implicated two gene families, the tryptophan amino transferase of *Arabidopsis* (TAA) family and the YUCCA (YUC) family of flavin monooxygenases, in auxin biosynthesis (Woodward and Bartel 2005, Mashiguchi et al. 2011). Mashiguchi et al. (2011) reported that the TAA family is involved in the production of indole-3-pyruvic acid (IPA) from tryptophan, and the YUC family functions in the conversion of IPA to IAA. IAA exists in two principal forms: a) free IAA, which is the bioactive form; and b) conjugated to sugars, myoinositol, amino acids or small peptides. Local concentrations of free IAA are regulated by the interplay of biosynthesis, formation of conjugates, hydrolysis of conjugates to free IAA, and transport (Woodward and Bartel 2005).

Auxin is redistributed throughout all aerial and underground plant body through fast, non-polar transport in phloem, and slow, cell-to-cell polar auxin transport (Figure 1). Several *Arabidopsis* mutants are defective in proteins mediating polar auxin transport (PAT). Among them, AUX1 mediates influx of IAA into cells (Marchant et al. 1999). In contrast, the PIN-FORMED (PIN) family of proteins is involved in polar auxin efflux (Woodward and Bartel 2005).
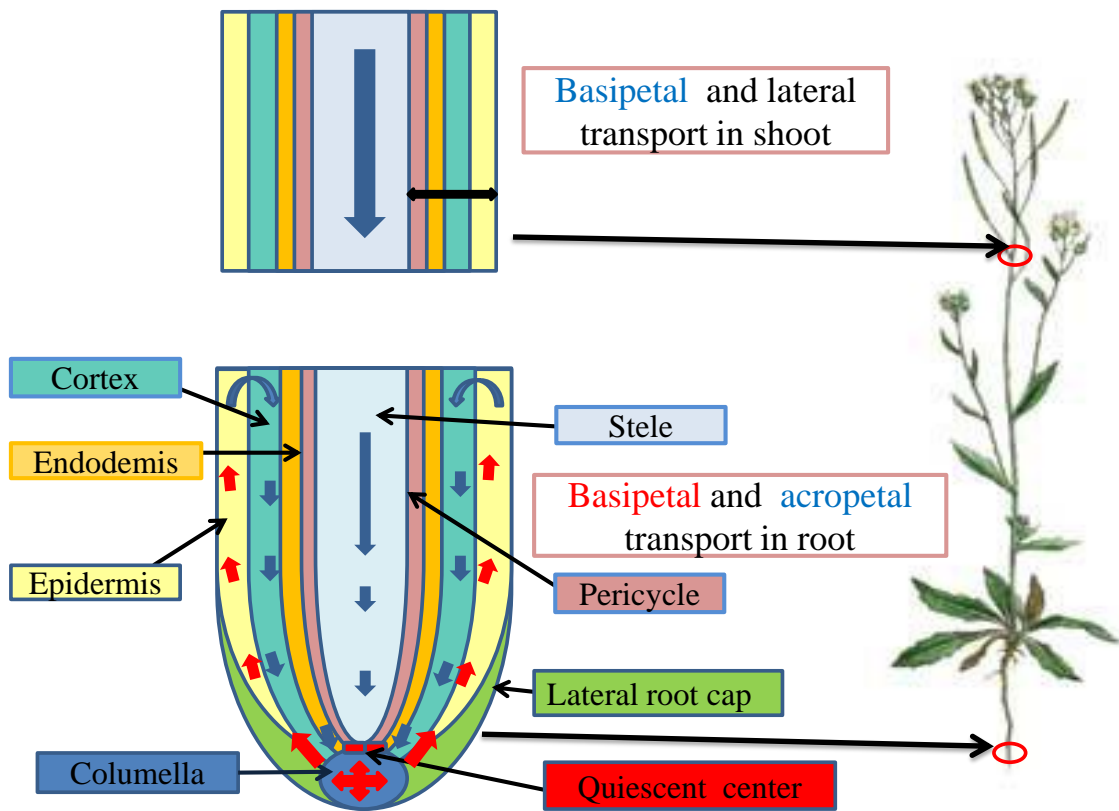

Figure 1. Transport of auxin in *Arabidopsis*. Auxin is transported from the aerial apical tissues towards the base through the vasculature (basipetaly). This stream passes the shoot-root junction, and it is further transported acropetaly in a rootward direction in the stele in the root. At the root tip, auxin redistributes, and then it is transported basipetaly in a shootward direction through the lateral root cap and epidermis into the root elongation zone where it can be recycled back into the vasculature stream. In the shoot, also exists a lateral transport of auxin between the main basipetal stream and outer cell layers.

The *aux1* loss-of-function mutations confer agravitropic phenotype, and resistance to auxin and ethylene in roots (Marchant et al. 1999). In contrast, the *eir1* loss-of-function mutants displayed agravitropic root growth and were less sensitive to ethylene inhibition than was root growth of wild type plants (Luschnig et al. 1998). AUX1 plays an important role in regulating the hormone flux between IAA source and sink tissues, thereby influencing lateral root development and root gravitropic responses (Marchant et al. 1999, Swarup et al. 2001, Marchant et al. 2002). The asymmetric localization of AUX1 and the auxin efflux transporter PIN1 to the upper and lower plasma membranes of protophloem cells has been proposed to promote the acropetal, post-phloem transport of auxin to the root apex (Swarup et al. 2001). On the other hand, it has been proposed that AUX1 and PIN2/EIR1 regulate root gravitropism by facilitating basipetal redistribution of auxin from the columella to distal elongation zone tissues via lateral root cap and epidermal tissues (Muller et al. 1998, Swarup et al. 2001). The polarity of basipetal transport in root is likely to be regulated by the apical plasma membrane localization of PIN2 in epidermal cells of the meristematic and elongation zones (Muller et al. 1998, Rahman et al. 2007). In contrast, the lack of polar localization of AUX1 in plasma membranes of lateral root cap and epidermal cells suggests that AUX1 does not actively direct the basipetal transport of auxin in roots (Swarup et al. 2001, 2004). On the other hand, PIN2 has a basipetal localization in cortical cells of the root elongation zone, and an acropetal localization in cortical cells of the meristem (Rahman et al. 2007). It is noteworthy to indicate that polar localization of PIN2 in cortical root cells has been proposed to represent a mechanism for fine-tuning the flow of auxin as required for optimal gravitropic responses (Rahman et al. 2010). Besides PIN proteins, multidrug resistance-like ABC transporters play also an important role in both acropetal and basipetal auxin transport (Wu et al. 2007).

The mechanism of auxin perception to transcriptional response acts trough alleviation of transcriptional repression (Figure 2). The current model proposes that under basal auxin conditions, a family of transcriptional repressors called AUX/IAAs bind to specific member of a family of transcriptional factors (ARFs), which show either repressor or activator activity. Increased auxin level facilitates the binding of the hormone to the F-box protein TIR1, a component of the E3 ubiquitin ligase complex SCF^{TIR1}, which triggers the ubiquitin-mediated proteolysis of AUX/IAA proteins. The destruction of AUX/IAA allows the release of ARFs and thereby triggers the auxin response (Woodward and Bartel 2005; Lau et al. 2008; Ruegger et al. 2012).
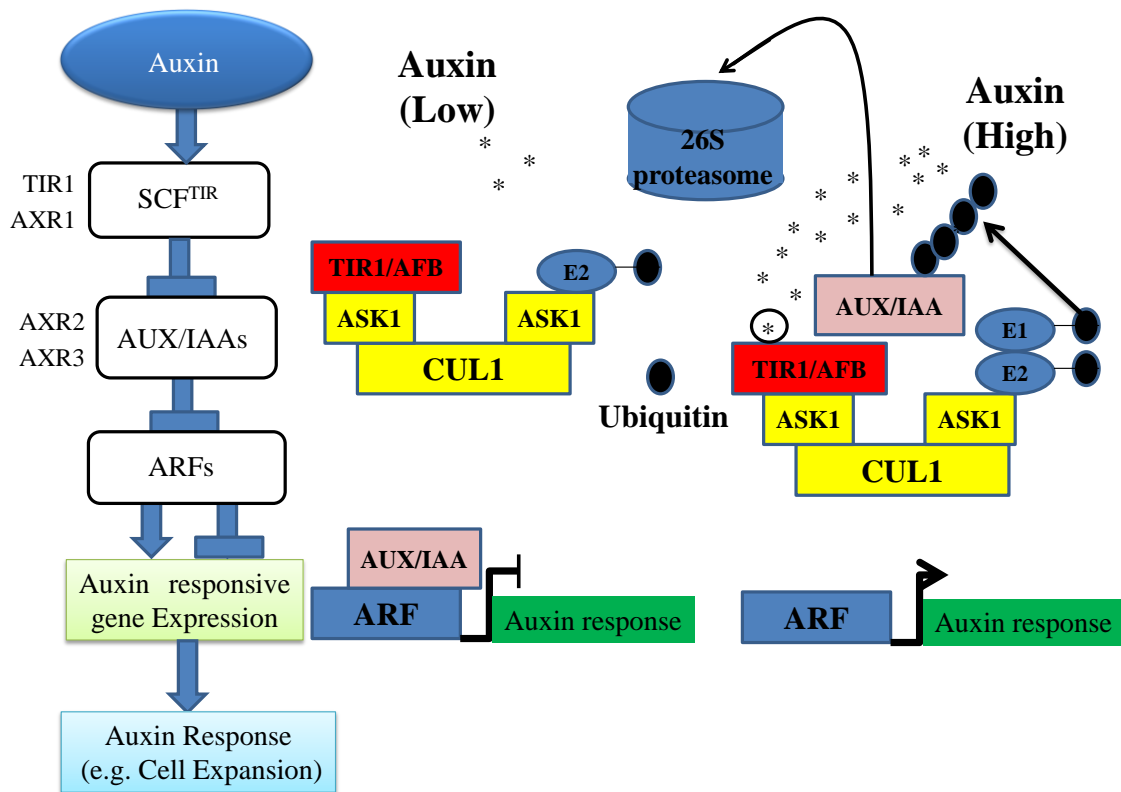

Figure 2. Auxin signaling.

ARFs, auxin response factors; AUX/IAAs, auxin/indole-3-acetic acid repressor proteins; ASK1, *Arabidopsis* serine/threonine kinase; CUL, cullin; E1: ubiquitin-activating enzyme; E2: ubiquitin-conjugating enzyme; SCF$^{TIR1/AFB}$, serine/threonine kinase-cullin-F-box protein complex; TIR1/AFB, *Arabidopsis* F-box proteins.

The *AXR1* gene encodes a protein related to the ubiquitin-activating enzyme (E1), the first enzyme in the ubiquitin conjugation pathway (Leyser et al. 1993). The *axr1* loss-of-function mutations confer auxin resistance to the root, and a variety of morphological defects including decreases in plant height, hypocotyl and stem elongation, irregular rosette leaves, and inflorescences more highly branched (Leyser et al. 1993). The semidominant *tir1-1* mutant displays increased root growth on medium containing either auxins or auxin transport inhibitors (Ruegger et al. 2012). On the other hand, dominant gain-of-function mutations in *AXR2* (*AUX/IAA17*) cause auxin and ethylene-resistant root growth, agravitropic root growth, a short hypocotyl and stem, and rosette leaves are small, round, and have a short petiole (Nagpal et al. 2000). Antiauxins such as *p*-chlorophenoxyisobutyric acid (PCIB) and yokonolide B (Ykb) inhibit the SCF^{TIR1} mediated auxin degradation of AUX/IAA proteins (Hayashi et al. 2003; Oono et al. 2003).

Microarrays analyses indicated that previously characterized auxin-responsive genes are not properly regulated when brassinosteroid (BR) biosynthesis is inhibited by brassinazole (Brz) (Chung et al. 2011). Besides, it has been published that the Auxin Response Element (AuxRE, TGTCTC) is enriched in genes regulated by both auxin and BR, which suggests that BRs and auxin signals converge at ARFs to regulate gene expression (Nemhauser et al. 2004; Goda et al. 2004). BRs induce early auxin-inducible genes (*IAA, SAUR-AC1*) and *DR5:GUS* without increasing the endogenous auxin levels per gram fresh weight (Nakamura et al. 2003a, b). The levels of the *IAA5, IAA19* transcripts were higher in wild type than in the BR-deficient mutant *det2*, even though IAA levels per gram fresh weight were lower in wild type seedlings (Nakamura et al. 2003a). AUX/IAA7 (AXR2) and AUX/IAA17 (AXR3) proteins are required for full BR induction of *IAA5* and *IAA9,* but they do not have a significant role in BR-mediated induction of *SAUR-AC1* (Nakamura et al. 2006). Besides, Nakamura et al. (2006) reported that Ykb inhibited both auxin, and BR-induced expression of *IAA5* and

SAUR-AC1, whereas PCIB only inhibited the auxin-induced expression of those genes. Based on these results, it was proposed that BR and auxin signaling pathways cross-talk downstream of auxin, somewhere between the site of PCIB and Ykb actions (Nakamura et al. 2006).

This work presents genetics and molecular evidences about the cross talk between BR and auxin during *Arabidopsis* root elongation. In order to broaden the spectrum of auxin mutants, we conducted a screen for auxin-hypersensitive (*axhs*) mutants selected on the basis of root phenotypes associated with auxin sensitivity. Characterization of the T-DNA insertional mutant *axhs1* indicates that *AXHS1* encodes DWF4, the rate limiting enzyme of BR biosynthesis (Choe et al. 1998). The *axhs1* mutant showed increased sensitivity to IAA, the synthetic auxin 2,4-dichlorophenoxyacetic acid (2,4-D), auxin transport inhibitors such as 2,3,5-triiodobenzoic acid (TIBA) and *N*-1-naphthylphthalamic acid (NPA), and the antiauxin PCIB. Genetic analyses of the interaction between the *axhs1* mutation and mutations affecting genes involved in auxin biosynthesis (*wei2-1*), auxin transport (*aux1-7, eir1-1*) and auxin signal transduction (*tir1-1, axr1-3, axr2-1*) indicate that auxin transport and functional components of the auxin-signaling pathway are required for the auxin-hypersensitive phenotype of *axhs1*. In addition, analysis of the expression of the *DR5:GUS* and *HS:AXR3NT-GUS* reporter genes in wild type and *axhs1* genotypes indicates that the *axhs1*mutation alters auxin responsiveness.

Materials and Methods

Plant materials and growth conditions

The *dwf4-102* (SALK_020761)*, dwf4-103* (SAIL_882_F07)*, tir1-1, axr1-3, axr2-1, eir1-1, aux1-7, wei2-1, det2, bri1-6* mutants*, DR5:GUS, HS:AXR3NT-GUS,* and *ASA1:GUS* transgenic lines were obtained from the Arabidopsis Biological Resource Center (ABRC) at Madison, USA.

A. thaliana seeds were surface sterilized in a mixture of 17% sodium hypochlorite (v/v) and 4% triton-X (v/v), and were allowed to germinate on plates containing *Arabidopsis* nutrient solution (Haughn and Somerville 1986), 1.5% sucrose and 1% agar. Plates were routinely kept in the dark for 2 days at 4°C to break seed dormancy, and then incubated in a near vertical position at 23°C with a 16 hour light/8 hour dark cycle. Unless otherwise indicated, seedlings were grown under light conditions. For dark conditions, plates were wrapped in three layers of aluminum foil. Day 0 of grow is defined as the time when plates were transferred to 23°C. Plants were grown to maturity on metromix 350.

Growth assays

Seedlings were germinated and grown for 7 days on solid media supplemented with or without the corresponding growth regulators. Final concentration of IAA, 2,4-D, and NAA ranged from 30 to 180 nM; BR concentration ranged from 0.1 to 10 nM; TIBA, and NPA concentration was 2,5 and 5 μ M; and PCIB concentration ranged from 5 to 15 μ M. Lengths of the root and hypocotyl of 20-25 seedlings were measured with a graduated ruler.

Isolation of axhs T-DNA insertion mutants

The *axhs1* mutant was isolated from an *Arabidopsis* transgenic plant collection (ecotype Columbia, Col, Alonso et al. 2003) available at ABRC.

Thermal asymmetric interlaced (TAIL-) PCR cloning of the AXHS1 gene

TAIL-PCR analysis was performed as described by Liu et al. (1995). The T-DNA insertion point was determined by sequencing the putative T-DNA-*AXHS1* tertiary PCR products identified in the analysis.

RNA isolation and RT-PCR analysis

Total RNA was isolated using RNeasy mini kit (Qiagen, Germany) following manufacturer's instructions. First strand cDNA was synthesized from about 1 μg total RNA from 7-day-old *Arabidopsis* seedlings, using PrimeScriptTM first strand cDNA synthesis kit (Takara, Japan) as described by the manufacturer. PCR was carried out under standard conditions, using axhs5-3 (5'-AGCACTCAAAGATGTTCGGTACA-3') and axhs3-6 (5- CCCTAATAGGCAAACCGTTAGGA -3') primers, which leads to the amplification of a 365 bp *DWF4* cDNA fragment. A 516 bp *AUX1* cDNA fragment, and a 422 bp *PIN2/EIR1* cDNA fragment were amplified using primer sets AUX1 (5'-ATGTCGGAAGGAGTAGAAGCGA-3' and 5'-GTTCTCTTGTCCAGATGATCG T-3'), and PIN2/EIR1 (5'-ATGATCACCGGCAAAGACATGT-3' and 5'- CTCTGA AGCACCACGATCTGCA-3'), respectively. The primer set Act2 (5'-GTTGGTGATGA AGCACAA-3' and 5'-CAAGACTTCTGGGCATCT-3') was used to amplify a 425 bp fragment of *Actin2* cDNA as an internal standard of gene expression.

Genetic crosses

Double mutants were selected in F2 populations by genotyping analysis, and the homozygous double mutants in the F3 generation were used for phenotypic analysis. GUS reporters (*DR5:GUS, HS:AXR3NT-GUS*) were introduced into the *axhs1* mutant background by crossing.

The genotype of the *axhs1-1* mutant was confirmed by genomic PCR analysis using the T-DNA left border primer LBa1 (5'-TGGTTCACGTAGTGGGCCATCG-3') and *AUXS1/DWF4* specific primers axhs5-3 and axhs3-3 (5'-AGCACTCAAAGATGTTCG GTACA-3') (Figure 3A). The presence of the GUS transgene was verified using gusF (5'-ATCGTGCTGCGTTTCGATGCGGT-3') and gusR (5'-AGGTTAAAGCCGACAG CAGCAGT-3') as GUS specific primers. The *wei2-1*, *axr1-3*, *axr2-1*, *tir1-1*, *eir1-1*, and *aux1-7* mutations were analyzed by using cleaved amplified polymorphic sequence (CAPS) markers (Figure 3B). The 269 bp PCR product amplified from *wei2-1* with wei2F (5'-GAATCCAAGTCCGTATATGGGTTATTTCTAG-3') and wei2R (5'-CGA TTCACTATCTTGTTCTGCTTCA-3'), and the 212 bp fragment amplified from *aux1-7* with aux1F (5'-ACCAACTTTGTTCGTCAAGTCGACACTCTAG-3') and aux1R (5'-AGCACGCATTTAAAGGGGTGTGT-3') were digested by XbaI in *wei2-1* and *aux1-7,* but they were not cleaved in wild type genotypes. On the other hand, there was an HaeIII site in the 204 bp PCR product amplified from wild type DNA with axr2.1F (5'-ACATGCGTACAAGCAAACATGA-3') and axr2R (5'-CACCACTACTGGTCTT CTGCTGA-3') primers, an NdeI site in the 209 bp fragment amplified from wild type DNA with axr1F (5'-GGTGGAAGATTCAATGTTGAAACTTGATAGCATAT-3') and axr1R (5'-GGCCAATATCCTAACCACGGCAT-3'), an NcoI site in the 231 bp PCR product amplified from wild type DNA with tir1F (5'-TCCTGCGAAGGCTTCTC CACCCATG-3') and tir1R (5'-GTATAATGAATATACAAATCACACACCA-3'), and a PstI site in the 225 bp fragment amplified from wild type DNA with eir1F (5'-TGCTTGATGTTGTTGATCATTTTATGCTGCA-3') and eir1R (5'-GCAATAAT CTTTGGTTGCAATGCCA-3'), that were absent in *axr2-1*, *axr1-3*, *tir1-1*, and *eir1-1* genotype*s*, respectively.
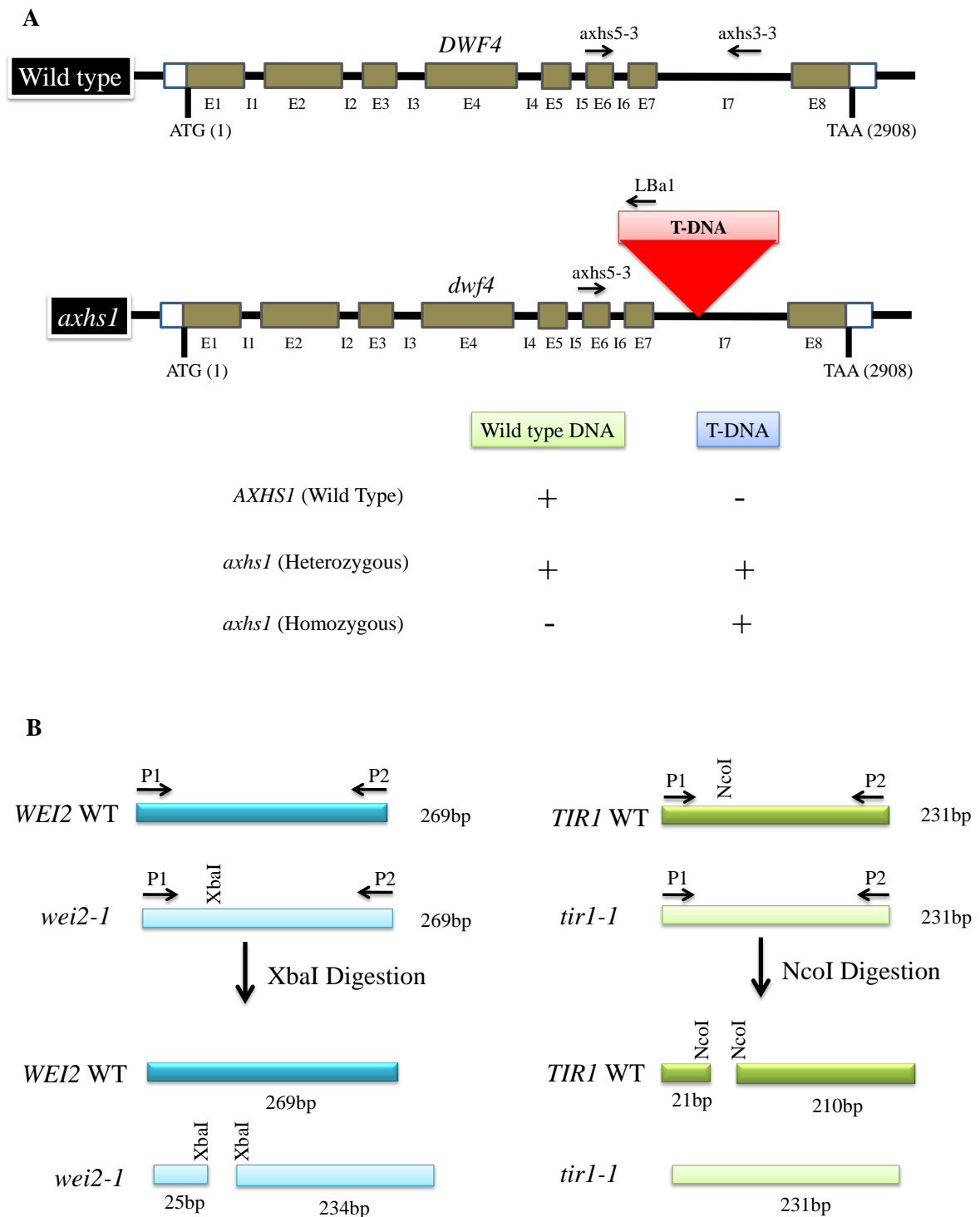
Figure 3. Mutant genotype analysis. (A) Analysis of the *axhs1* genotype by PCR
(B) Analysis of the *wei2-1* and *tir1-1* genotypes by CAPS markers. WT = Wild Type.

GUS expression analysis

Seven day-after-germination *DR5:GUS, axhs1 DR5:GUS, ASA1:GUS* and *axhs1 ASA1:GUS* seedlings were treated with growth regulators for 48 h and then incubated in GUS staining buffer containing 50 mM potassium phosphate buffer (pH 7), 20% (v/v) methanol, 10 mM EDTA, 0.5 mM potassium ferricyanide, 0.5 mM potassium ferrocyanide, 0.1% (v/v) Triton X-100 and 1 mM 5-bromo-4-chloro-3-indolyl-β-D-glucuronide (X-Gluc) at 25°C for 20 h. Samples were then incubated sequentially in 90%, 80%, and 70% ethanol to remove plant pigments. After that, samples were whole mounted in chloral hydrate solution (8g of chloral hydrate, 1 mL of glycerol, and 2 mL of water) to enhance transparency of the tissue.

Protein stability assays

Seven day-after-germination *HS:AXR3NT-GUS* and *axhs1 HS:AXR3NT-GUS* seedlings were submerged into liquid medium and heat shocked for 2 h at 37°C. After that, seedlings were transferred to fresh medium for 20 min, treated for 10-105 min in medium supplemented with growth regulators, and stained with X-gluc for 20 h as described above.

Results

Isolation of the axhs1 mutant

In order to identify new genes involved in auxin response we screened 3,300 T-DNA transformed lines of ecotype Columbia (Col) for seedlings with an increased sensitivity to 2,4-D for the root elongation response. One mutant line (*axhs1*) was selected as an auxin-hypersensitive mutant (Figure 4A). The roots of *axhs1* seedlings grown in control and auxin-containing media were somewhat shorter than those of the wild type, but the main characteristic of the *axhs1* mutant is a short hypocotyl in seedlings grown under both light and dark conditions (Figure 4 A-B, Figure 5, Figure 12A).
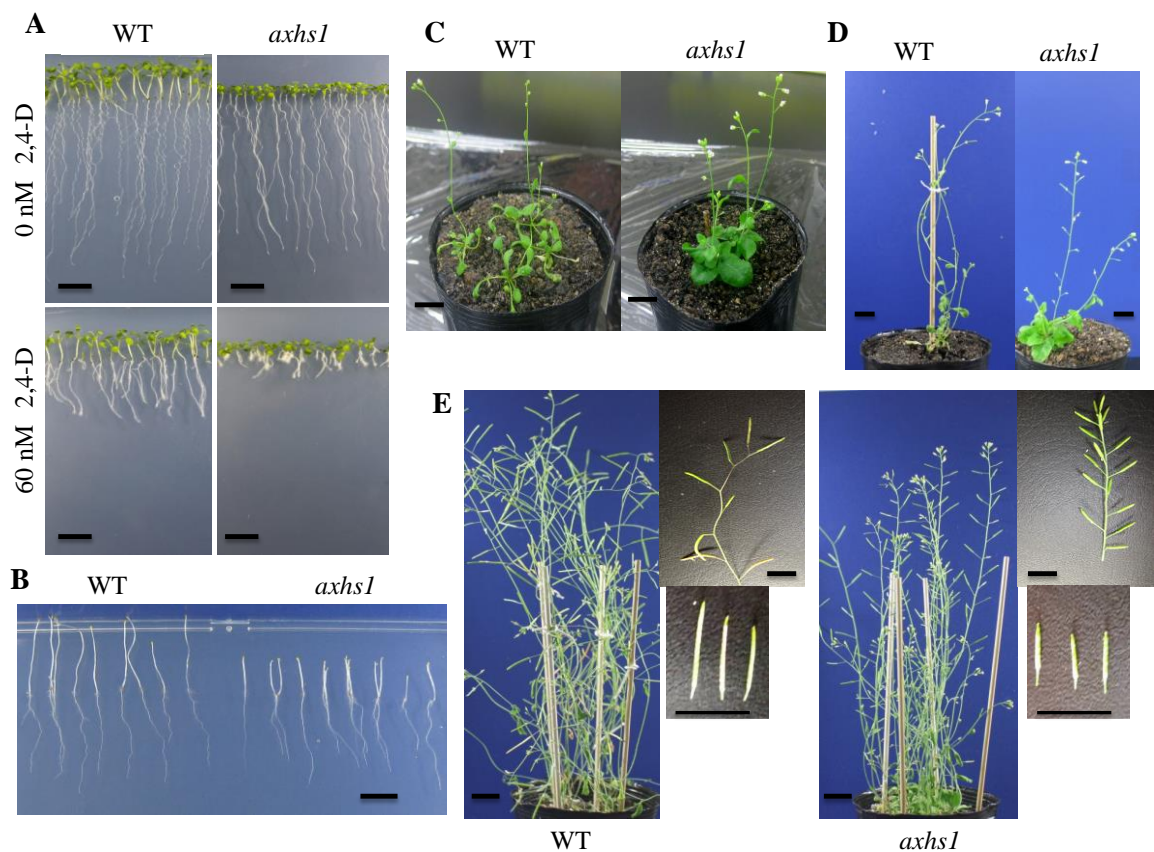

Figure 4. Comparison of the auxin sensitivity and morphology of wild type (Col) and *axhs1* mutant plants. (A) Phenotypes of seedlings grown for 7 days on 0 and 60 nM 2,4-D. (B) Seven-day-old etiolated seedlings. Morphology of plants at 21 (C), 28 (D), and 44 days (E). Insets show a magnified view of siliques. Bars = 1cm.

Mature *axhs1* plants showed a weak dwarf phenotype. The height of *axhs1* plants was reduced compared to wild type (Figure 4C-E, Figure 5 Figure 12B). Besides they exhibited round rosette leaves with short petioles (Figure 4C-D), and a large number of siliques which were smaller compared to those of the wild type (Figure 4D-E, Figure 5).
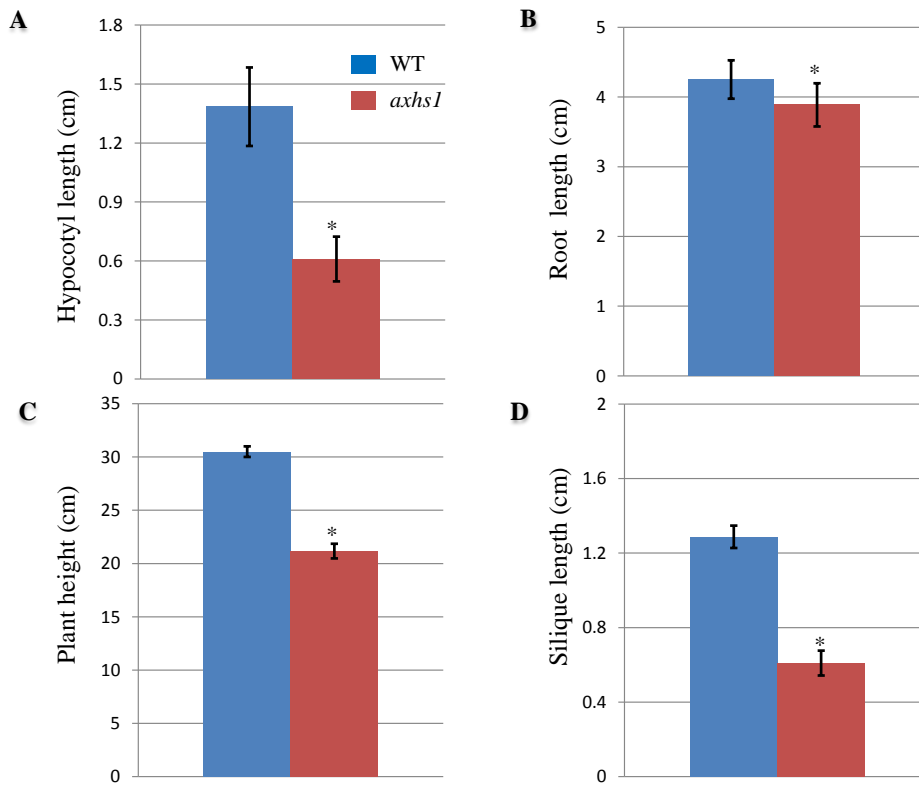

Figure 5. Phenotypes of *axhs1* plants. A) Hypocotyl length of wild type and *axhs1* seedlings grown for 7 days in the dark. Average and SD of the hypocotyl length of more than 20 seedlings are shown. B) Root length of 7-day-old wild type and *axhs1* seedlings. Data represent mean $\pm$ SD of more than 30 seedlings from at least two independent experiments. C) Height of wild type and *axhs1* plants grown for 6 weeks. Average and SD of the height of 10-12 plants are shown. D) Silique length of 6-week-old wild type and *axhs1* plants. Average and SD of the length of more than 25 siliques are shown. An asterisk indicates a significant difference from wild type by Student's t-test ($p < 0.05$).

Root elongation in axhs1 is hypersensitive to auxins, antiauxins, and auxin transport inhibitors

In order to characterize the response of *axhs1* to auxin and related compounds, wild type and *axhs1* seeds were germinated directly on growth medium supplemented with the compound of interest and root length was scored after 7 days. The *axhs1* mutant

showed increased sensitivity to IAA, the synthetic auxin 2,4-D, auxin transport inhibitors such as TIBA and NPA, and the antiauxin PCIB (Figure 6). In contrast, the roots of *axhs1* showed will type sensitivities to the synthetic auxin NAA (Figure 6), the ethylene precursor (1-amino-cyclopropane-1-carboxylic acid) ACC, and kinetin (data not shown). These results suggest that AXHS1 is involved in auxin transport and/or signal transduction.
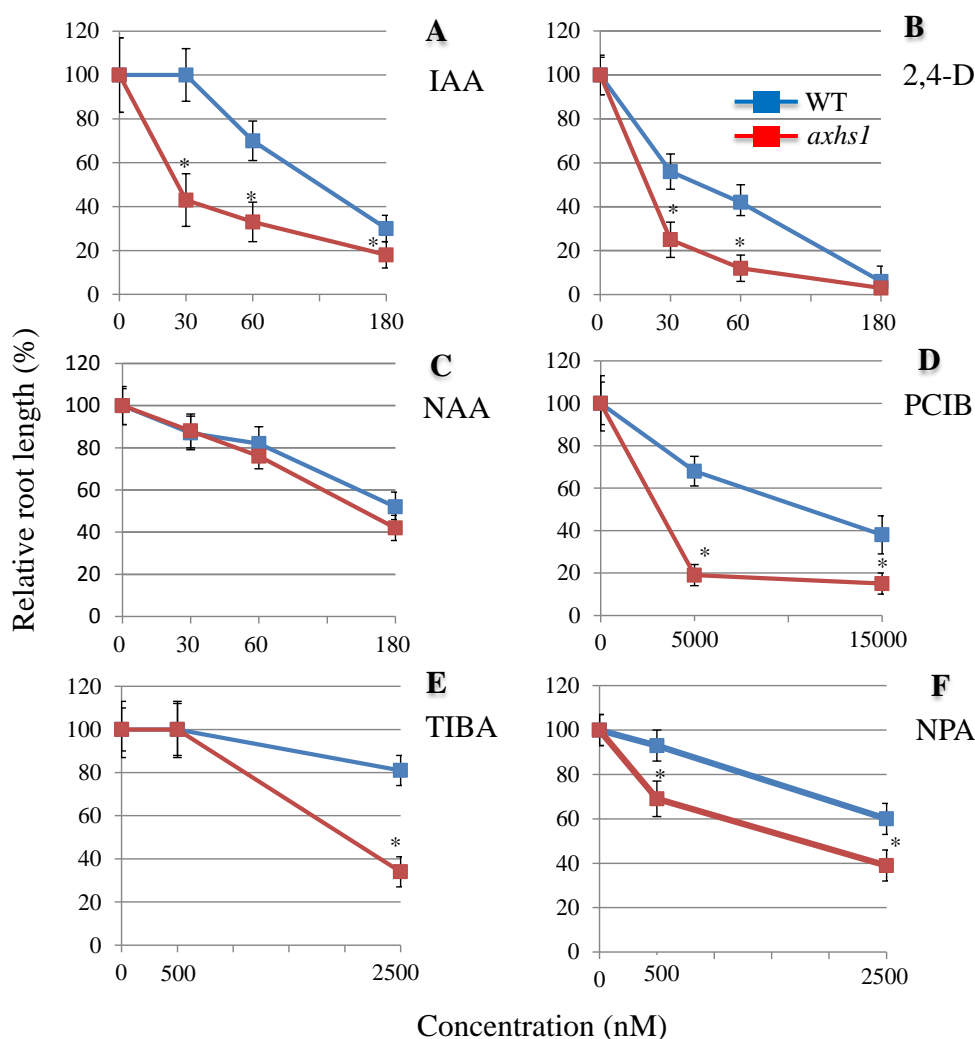

Figure 6. *axhs1* is hypersensitive to auxins, antiauxins, and auxin transport inhibitors. Dose-response curves of roots of 7-day-old wild type and *axhs1* seedlings grown in solid medium supplemented with or without IAA (A), 2,4-D (B), NAA (C), PCIB (D), TIBA (E), NPA (F). Relative root length is expressed as a percentage of the length observed in unsupplemented medium. Values are means $\pm$ SD of at least two independent experiments in which root length of 20-25 seedlings was measured. An asterisk indicates a significant difference from wild type by Student's t-test ($p<0.05$).

17

axhs1 is a weak allele of DWF4

TAIL-PCR analysis indicated the presence of a T-DNA inserted in intron 7 of the *DWF4 (DWARF4)* gene in *axhs1* (Figure 7A). *DWF4* encodes a C-22 hydroxylase that is crucial for BR-biosynthesis and the feedback control of endogenous BR levels (Choe et al. 1998; Yoshimitsu et al. 2011). Since the T-DNA insertion was found in intron 7, the *axhs1* gene might produce a wild type DWF4 protein and/or a non-functional protein lacking the conserved heme-binding domain (Figure 7A-B). The proposed brassinosteroid biosynthesis pathway is illustrated in Figure 8.

The expression of *DWF4* in *axhs1* was analyzed by RT-PCR, using primers designed for amplification of a 365 bp cDNA fragment including part of exon 6 and 8 (Figure 7A). RT-PCR analysis indicated that *axhs1* showed low levels of mature *DWF4* mRNA accumulation compared to wild type (Figure 7C). The identity of spliced *DWF4* cDNA was verified by cDNA sequencing.

We crossed *axhs1* with wild type Col and analyzed 62 plants from the F2 generation. Results indicated that the *axhs1* phenotypes, including auxin hypersensitivity and short hypocotyl (Figure 7D), were caused by a single recessive mutation linked to the T-DNA insertion in the *DWF4* gene. In order to confirm that the *axhs1* phenotypes are caused by a T-DNA insertion in DWF4 we analyzed other *dwf4* alleles of the Col ecotype. *dwf4-102* is a strong mutant allele with a T-DNA inserted in exon 5 of *DWF4* (Nakamoto et al. 2006). We searched for other *dwf4* alleles and found a line (SAIL_882_F07 = *dwf4-103*) carrying a T-DNA insert in intron 7 of *DWF4* (Figure 7A). The phenotype of *axhs1* and *dwf4-103* plants was quite similar (data not shown), and clearly resembled that of weak alleles of *DWF4* (Nakamoto et al. 2006). Moreover, as illustrated in Figure 7E, *dwf4-102* and *dwf4-103* had a level of sensitivity to 2,4-D similar to that of *axhs1*. On the other hand, we carried out a complementation test between *axhs1* and *dwf4-102*. Since strong mutant alleles of *DWF4* are infertile (Azpiroz et al. 1998; Nakamoto et al. 2006), heterozygous *dwf4-102* was crossed with *axhs1*. Analysis of the F1 and F2 segregation indicated that *axhs1* is allelic to *dwf4-102* (Figure 7F). Thus, hereafter, *axhs1* will be named *axhs1/dwf4*.
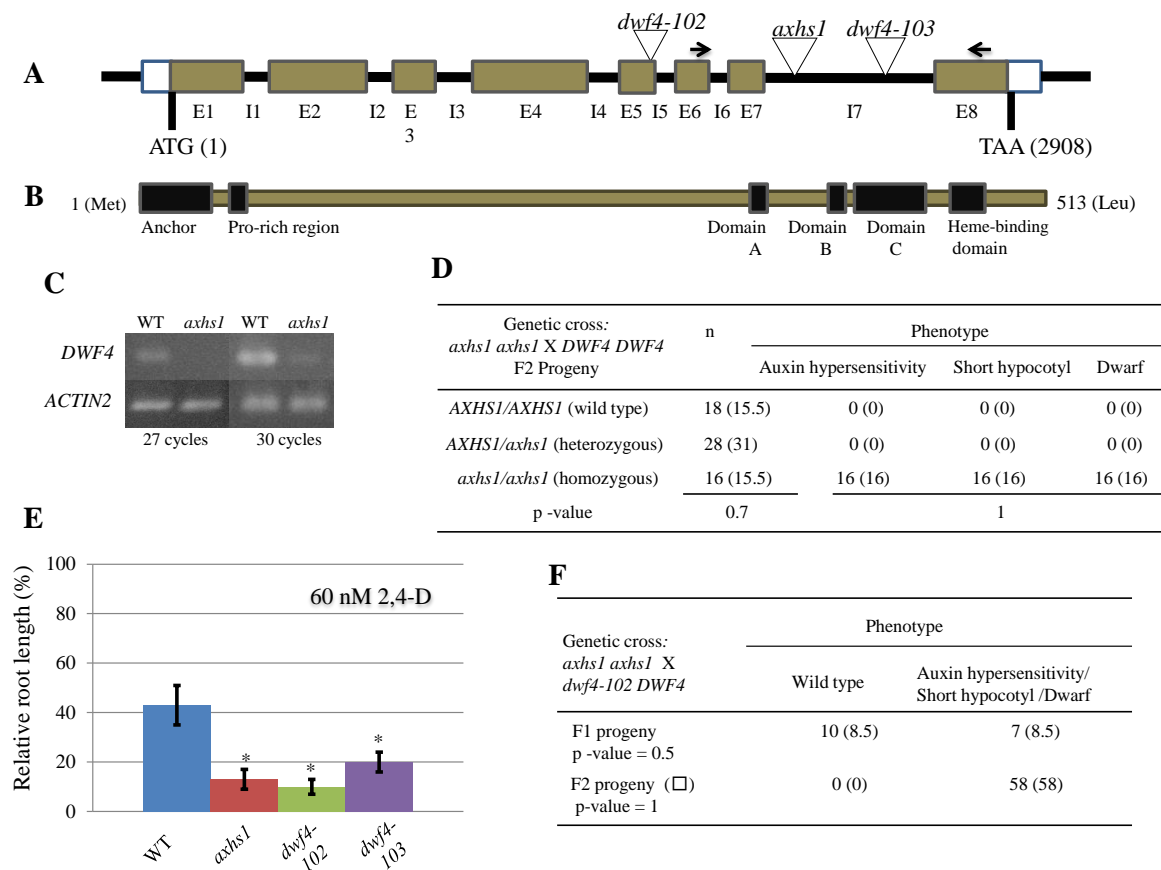
Figure 7. TAIL-PCR cloning of *AXHS1/DWF4*: *ahxs1* is a weak allele of *DWF4* gene. (A) Genomic structure of the *DWF4* gene. Rectangles and lines represent exons and introns, respectively. Triangles indicate the position of T-DNA insertions. Arrows indicate the primers used in RT-PCR expression analysis in (C). (B) Major domains of the DWF4 protein (Choe et al. 1998). (C) RT-PCR analysis. Seven-day-old wild type and *axhs1* seedlings were analyzed for expression of *DWF4*. The number of PCR cycles is indicated. The figure illustrates representative results from three independent experiments. (D) F2 progeny from the cross between wild type and *axhs1* was analyzed for *axhs1* phenotypes. Auxin sensitivity was determined in seedlings grown in solid medium supplemented with 60 nM 2,4-D for 7 days. Genotypes were verified by genomic PCR using axhs5-3, axhs3-3, and LBa1 primers. p = value of Chi-square test. The expected data, which are written in parenthesis, were calculated on the assumption that auxin hypersensitivity, short hypocotyl and dwarf phenotypes are caused by a single recessive mutation. n = number of plants analyzed. (E) *dwf4* mutants are hypersensitive to auxin. Wild type, *axhs1, dwf4-102* and *dwf4-103* seedlings were grown for 7 days in solid medium supplemented with or without 60 nM 2,4-D. Root length is expressed relative to untreated seedlings. Average and SD of more than 20 seedlings are shown. An asterisk indicates a significant difference from wild type by Student's t-test ($p<0.05$). (F) Progeny from the cross between *axhs1* (homozygous) and *dwf4-102* (heterozygous) was evaluated for auxin sensitivity, short hypocotyl, and dwarf phenotypes as indicated in (C). □= The progeny from 4 independent F1 plants exhibiting auxin hypersensitivity, short hypocotyl, and dwarf phenotypes was analyzed.　p = value of Chi-square test. The expected data, which are written in parenthesis, were calculated on the assumption that *axhs1* and *dwf4-102* are allelic mutations.
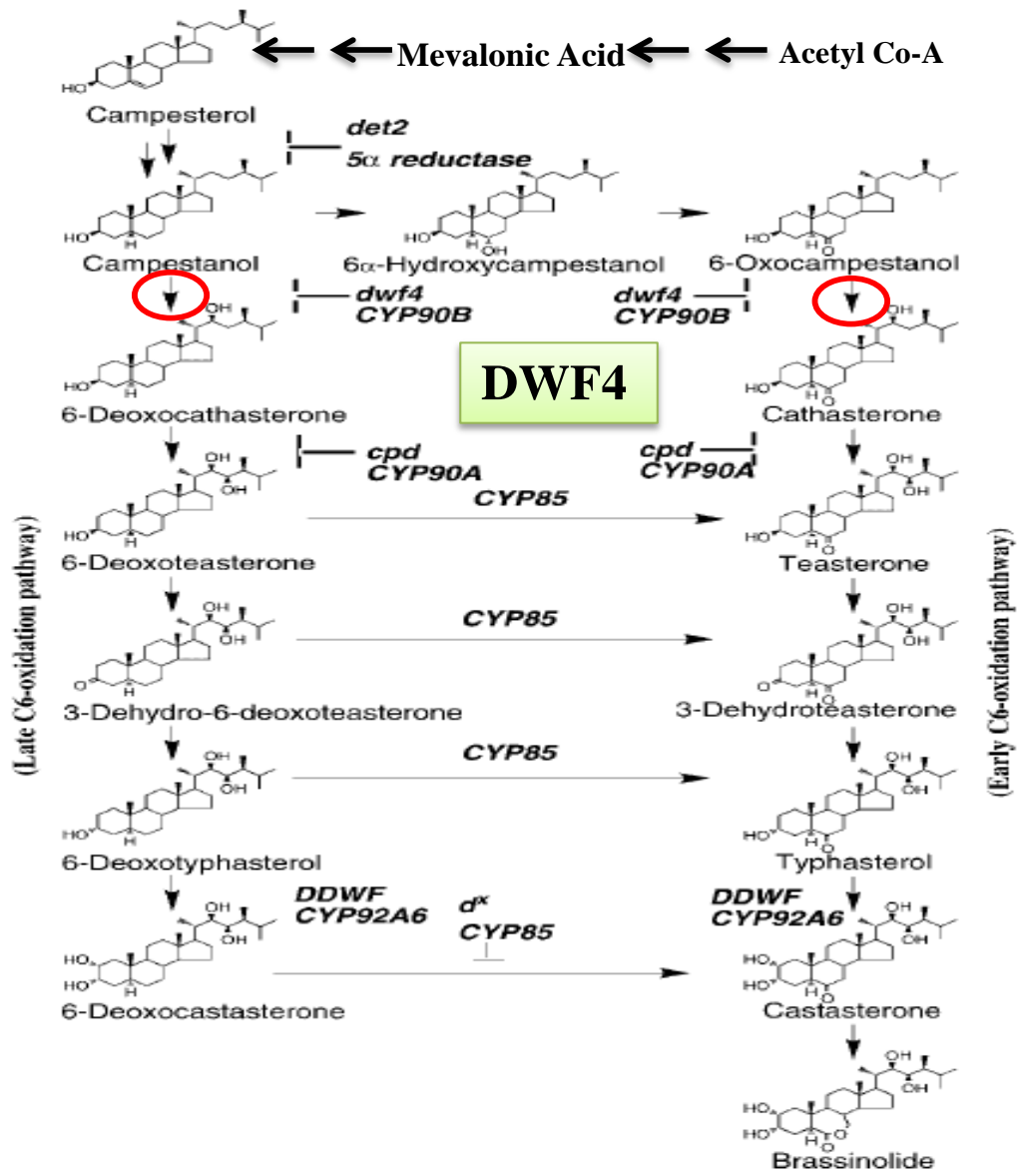
19

Figure 8. Proposed brassinosteroid biosynthesis pathway in plants (adapted from Choe et al. 1998).

In order to verify the cross talk between auxin and BR, we examined whether the short hypocotyl and auxin hypersensitivity of *axhs1/dwf4* could be rescued by exogenous application of BR. As shown in Figure 9, the short hypocotyl of *axhs1/dwf4* was partially rescued by addition of 10 nM brassinolide (BL) (Figure 9A). On the other hand, 0.1 nM BL promoted root growth in wild type and *axhs1* seedlings grown in auxin-free medium (Figure 9B). Besides, the inhibition of root growth by 2,4-D in wild type and *axhs1* seedlings was rescued by BL (Figure 9B). These results confirm that *axhs1/dwf4* is a BR-deficient mutant, and suggest that BRs negatively regulate auxin sensitivity in roots.
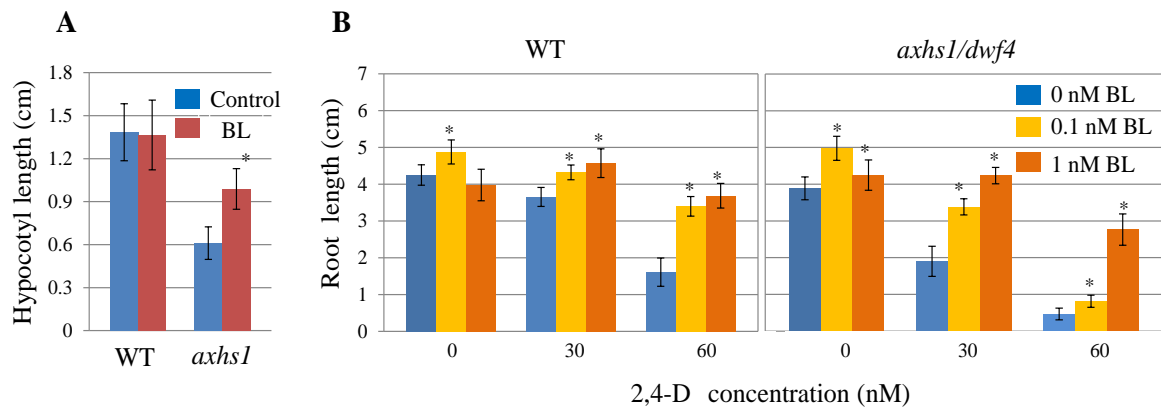

Figure 9. The short hypocotyl and auxin hypersensitive phenotypes of *ahxs1* are rescued by BL. A) Wild type and *axhs1/dwf4* seedlings were grown for 7 days in the dark in medium supplemented with and without 10 nM BL. B) Wild type and *axhs1* seedlings were grown for 7 days on 0, 30, and 60 nM 2,4-D medium supplemented with 0, 0.1, and 1 nM BL. Average and SD of the root and hypocotyl length of more than 20 seedlings are shown. An asterisk indicates a significant difference from BL-free medium supplemented with 0, 30, or 60 nM 2,4-D, by Student's t-test ($p<0.05$).

Genetic interaction between axhs1/dwf4 and auxin mutants

Our data indicate that *axhs1* is a *dwf4* mutant allele that is hypersensitive to auxins, the antiauxin PCIB and auxin transport inhibitors such as TIBA and NPA. In order to analyze the impact of the *axhs1/dwf4* mutation on auxin biosynthesis, transport, and signaling, we constructed and characterized double mutants between *axhs1/dwf4* and mutants affected in auxin biosynthesis (*wei2-1*), auxin transport (*aux1-7, eir1-1*), and auxin signal transduction (*tir1-1, axr1-3, axr2-1*).

In order to construct a mutant defective in both BR (*axhs1/dwf4)* and auxin (*wei2-1*) biosynthesis, *axhs1/dwf4* and *wei2-1* mutants were crossed, and F2 progeny analyzed by PCR (Figure 10) as described in Materials and Methods. Plant number 1 and 7 were selected as double mutants.
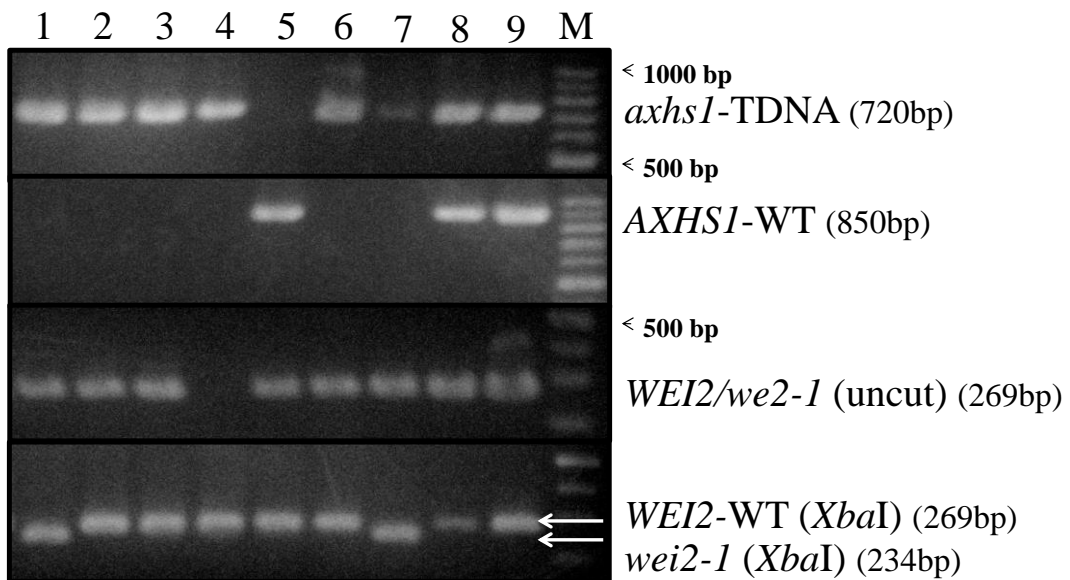

Figure 10. Construction of the *axhs1/dwf4 wei2-1* double mutant. Genomic DNA from F2 progeny of the cross between homozygous *axhs1* and *wei2-1* was isolated, and analyzed by PCR as described in Materials and Methods. 1) homozygous *axhs1/dwf4* homozygous *wei2-1,* 2) homozygous *axhs1/dwf4* wild type *WEI2,* 3) homozygous *axhs1/dwf4* wild type *WEI2,* 4) homozygous *axhs1/dwf4* wild type *WEI2,* 5) wild type *AXHS1/DWF4* wild type *WEI2,* 6) homozygous *axhs1/dwf4* wild type *WEI2,* 7) homozygous *axhs1/dwf4* homozygous *wei2-1,* 8) heterozygous *axhs1/dwf4* wild type *WEI2,* 9) heterozygous *axhs1/dwf4* wild type *WEI2.*

The *axhs1 wei2-1* mutant exhibited levels of IAA, 2,4-D, NPA and PCIB sensitivity (Figure 11) similar to those of the *axhs1/dwf4* mutant. It is noteworthy to indicate that *wei2.1* showed increased sensitivity to PCIB (Figure 11), which could be due to an altered ratio of the auxin-to-antiauxin signal in this mutant.
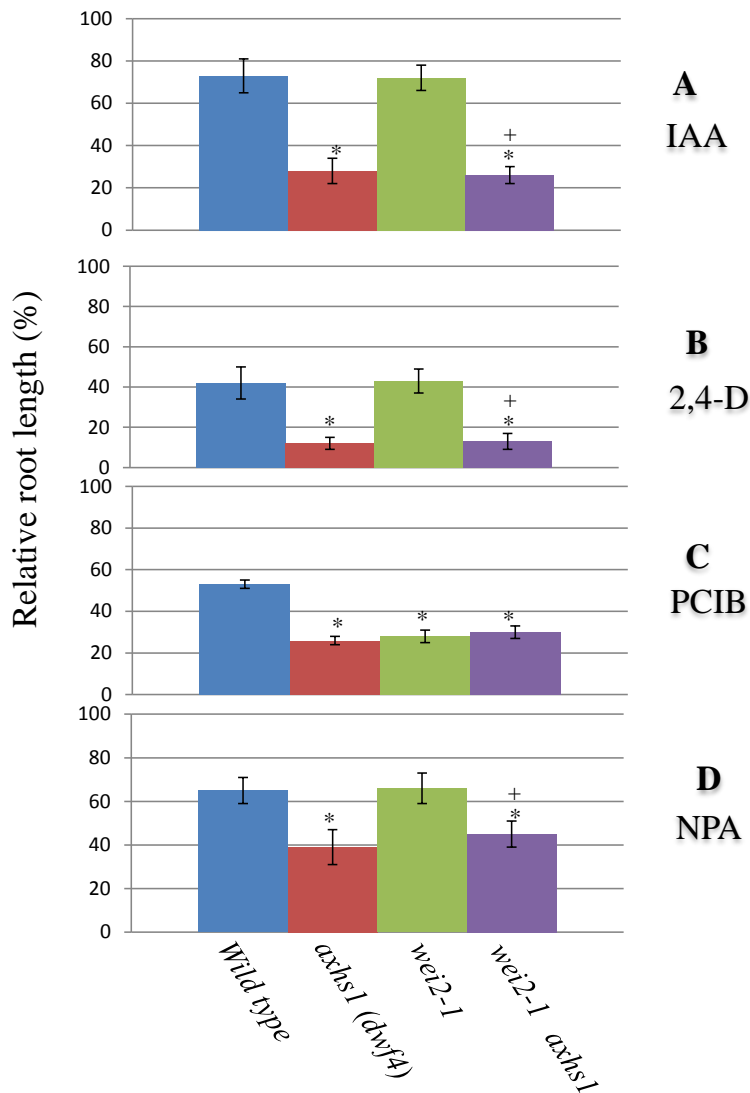
Figure 11. Interaction between *AXHS1/DWF4* and genes involved in auxin biosynthesis. Wild type, *axhs1*(*dwf4*), *wei2-1,* and *axhs1*(*dwf4*) *wei2-1* seedlings were grown for 7 days in control medium and 60 nM IAA, 60 nM 2,4-D, 10 μ M PCIB, or 2.5 μ M NPA containing medium. Relative root length is expressed as a percentage of the length observed in unsupplemented medium. Data represent mean $\pm$ SD of more than 20 seedlings from at least two independent experiments. * = significant difference from wild type by Student's t-test (p<0.05). + = significant difference from *wei2-1* by Student's t-test (p<0.05).

The morphology of the *axhs1/dwf4 wei2-1* mutant was indistinguishable from that of the *axhs1/dwf4* single mutant (Figure 12A, B). These results strongly suggest that endogenous auxin levels have no significant impact on the *axhs1/dwf4* mutant phenotypes.
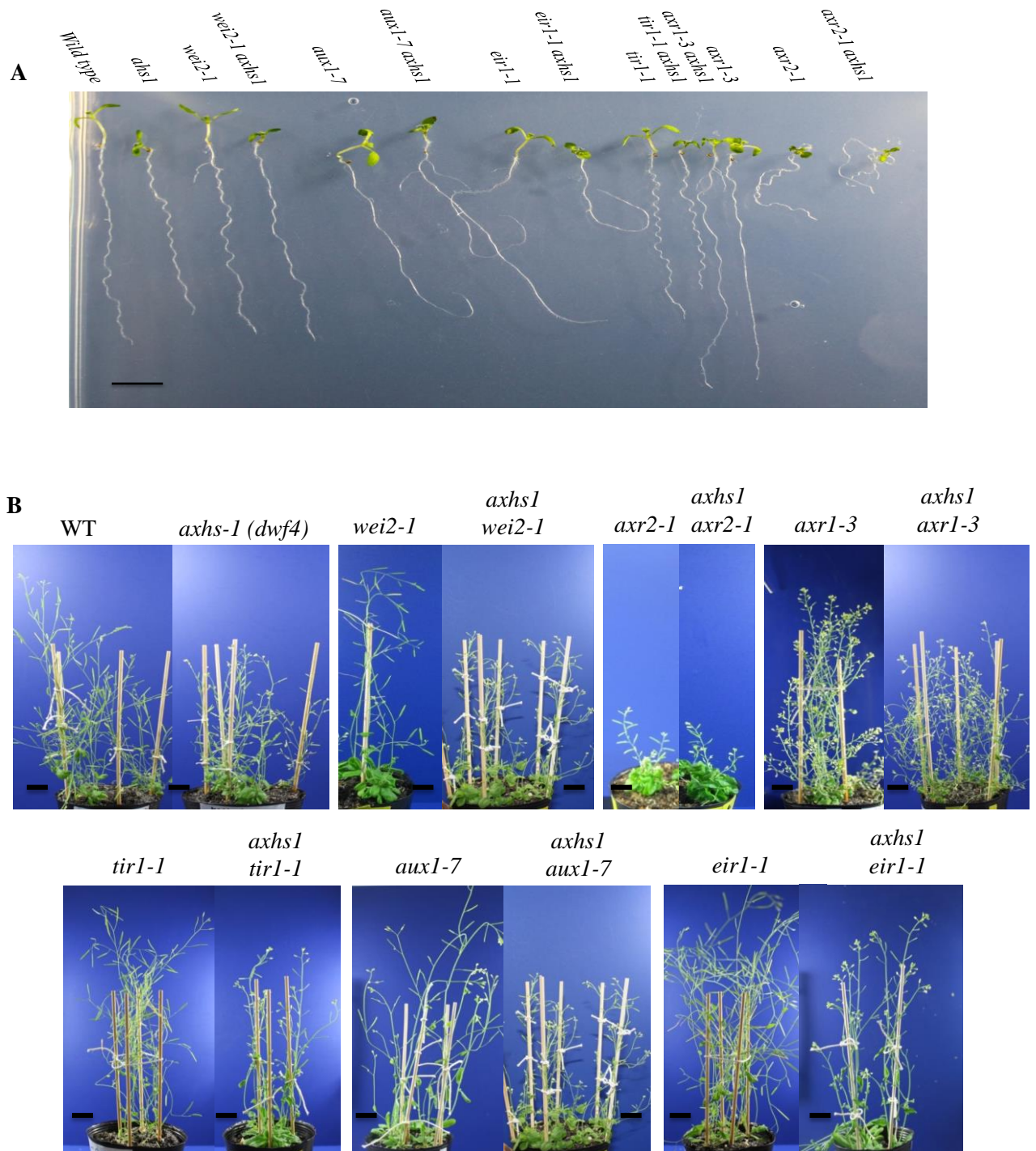
23

Figure 12. Phenotype of seedlings and mature plants. Wild type, *axhs1*(*dwf4*), *wei2-1, axhs1*(*dwf4*) *wei2-1, tir1-1*, *axhs1*(*dwf4*) *tir1-1*, *axr1-3*, *axhs1*(*dwf4*) *axr1-3*, *axr2-1*, *axhs1*(*dwf4*) *axr2-1*, *aux1-7*, *axhs1*(*dwf4*) *aux1-7*, *eir1-1*, and *axhs1*(*dwf4*) *eir1-1* plants were grown in solid medium for seven days (A), and in soil for 6 weeks (B). Bars = 1cm.

To further evaluate a possible role of BR in ASA1 (WEI2)-mediated auxin biosynthesis, the *ASA1:GUS* reporter gene (Stepanova et al. 2005) was introduced in the *axhs1/dwf4* background by genetic crosses, and its expression was examined. The expression of *ASA1:GUS* was not affected by BL treatment (Figure 13). Besides, no significant difference in GUS staining was observed between wild type and *axhs1/dwf4* seedlings treated with or without BL (Figure 13).
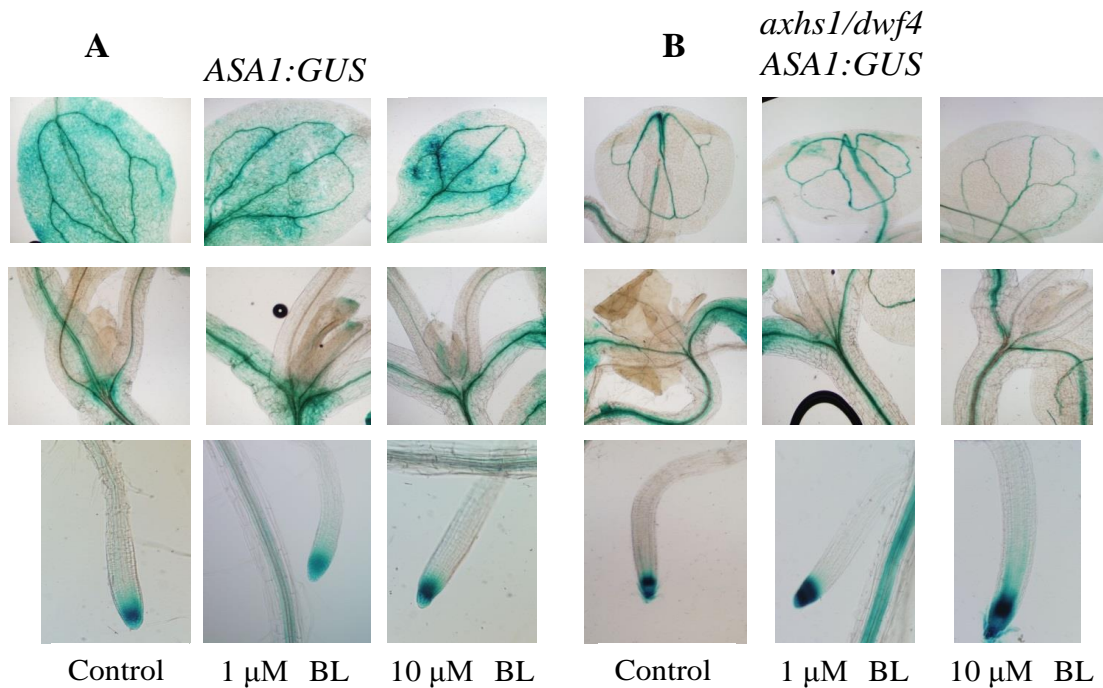

Figure 13. The *ASA1:GUS* reporter gene expression is not regulated by BRs. GUS activity was monitored in *ASA1:GUS* and *axhs1/dwf4 ASA1:GUS* seedlings grown in agar plates for 7 days and then incubated for 24 h in mock-treated liquid medium and liquid medium supplemented with BL. Seedlings were stained for GUS for 20 h, and representative seedlings from three independent experiments were photographed.

The *axhs1/dwf4 axr1-3* double mutant was constructed by genetic crosses. *axhs1/dwf4* and *axr1-3* mutants were crossed, and F2 progeny analyzed by PCR (Figure 14) as described in Materials and Methods.
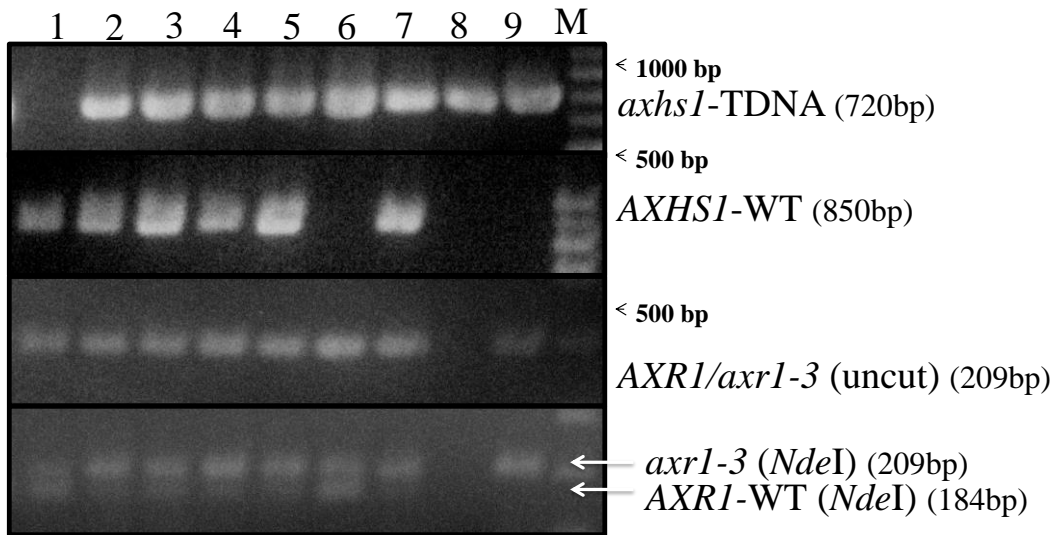

Figure 14. Construction of the *axhs1/dwf4 axr1-3* double mutant. Genomic DNA from F2 progeny of the cross between homozygous *axhs1/dwf4* and *axr1-3* was isolated, and analyzed by PCR as described in Materials and Methods. 1) wild type *AHS1/DWF4* heterozygous *axr1-3,* 2) heterozygous *axhs1/dwf4* heterozygous *axr1-3,* 3) heterozygous *axhs1/dwf4* heterozygous *axr1-3,* 4) heterozygous *axhs1/dwf4* heterozygous *axr1-3,* 5) heterozygous *axhs1/dwf4* heterozygous *axr1-3,* 6) homozygous *axhs1/dwf4* heterozygous *axr1-3,* 7) heterozygous *axhs1/dwf4* homozygous *axr1-3,* 8) homozygous *axhs1/dwf4* *axr1-3?,* 9) homozygous *axhs1/dwf4* homozygous *axr1-3.*

The *axr1-3* mutant showed increased resistance to NPA and PCIB compared to wild type seedlings (Figure 15). *axhs1/dwf4 axr1.3* had an intermediate sensitivity to IAA, 2,4-D, and NPA between wild type and *axr1-3,* but it had levels of resistance to 10μ M PCIB very similar to those of *axr1-3* (Figure 15).
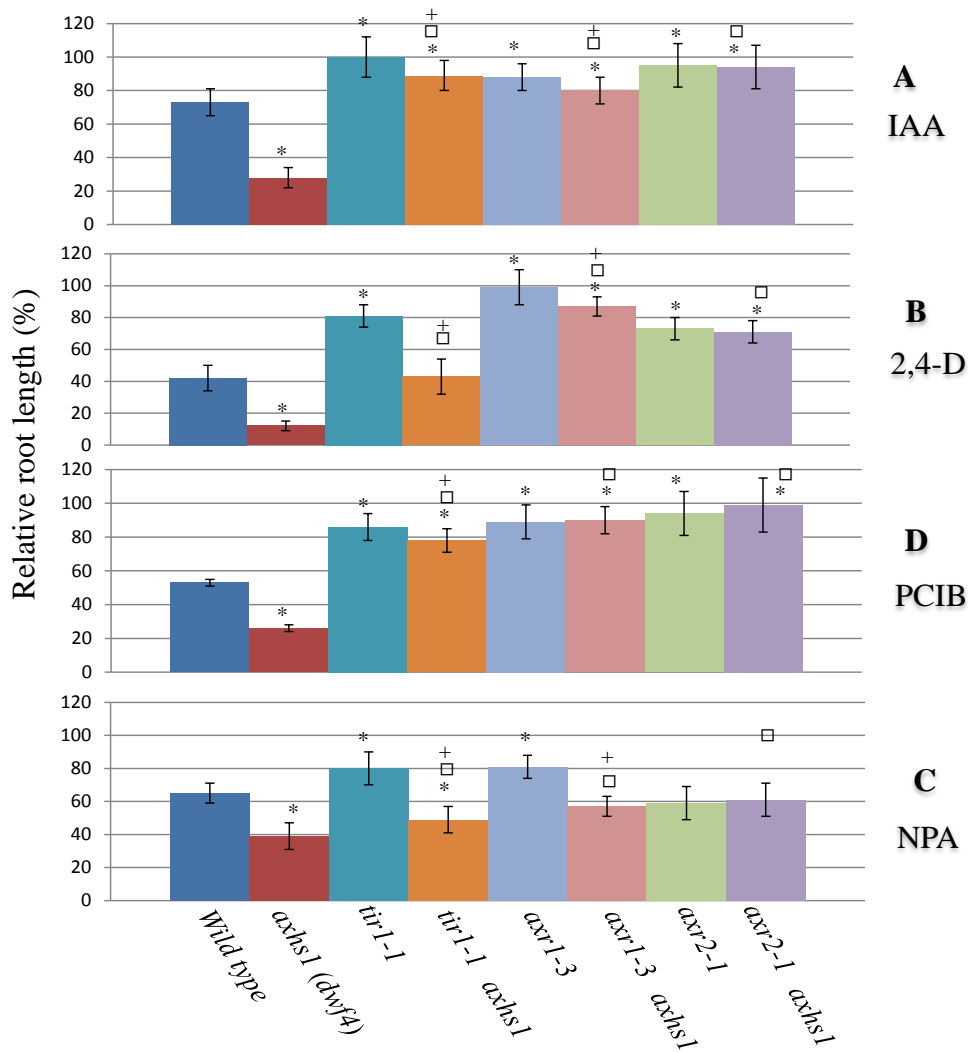
26

Figure 15. Interaction between *AXHS1/DWF4* and genes involved in auxin signal transduction. Wild type, *axhs1(dwf4)*, *tir1-1*, *axhs1(dwf4) tir1-1*, *axr1-3*, *axhs1(dwf4) axr1-3*, *axr2-1*, and *axhs1(dwf4) axr2-1* seedlings were grown for 7 days in control medium and 60 nM IAA, 60 nM 2,4-D, 10 μM PCIB, or 2.5 μM NPA containing medium. Relative root length is expressed as a percentage of the length observed in unsupplemented medium. Data represent mean $\pm$ SD of more than 20 seedlings from at least two independent experiments. * = significant difference from wild type by Student's t-test (p<0.05). □ = significant difference from *axhs1/dwf4* by Student's t-test (p<0.05). + = significant difference from *tir1-1*, *axr1-3*, or *axr2-1* by Student's t-test (p<0.05).

The morphology of the *axhs1/dwf4 axr1-3* mutant was indistinguishable from that of the *axr1-3* single mutant (Figure 12). These results suggest that *AXHS1/DWF4* functions at the level or downstream of *AXR1*.

We constructed an *axhs1/dwf4 tir1-1* double mutant by genetic crosses. *axhs1/dwf4* and *tir1-1* mutants were crossed, and F2 progeny analyzed by PCR (Figure 16) as described in Materials and Methods.
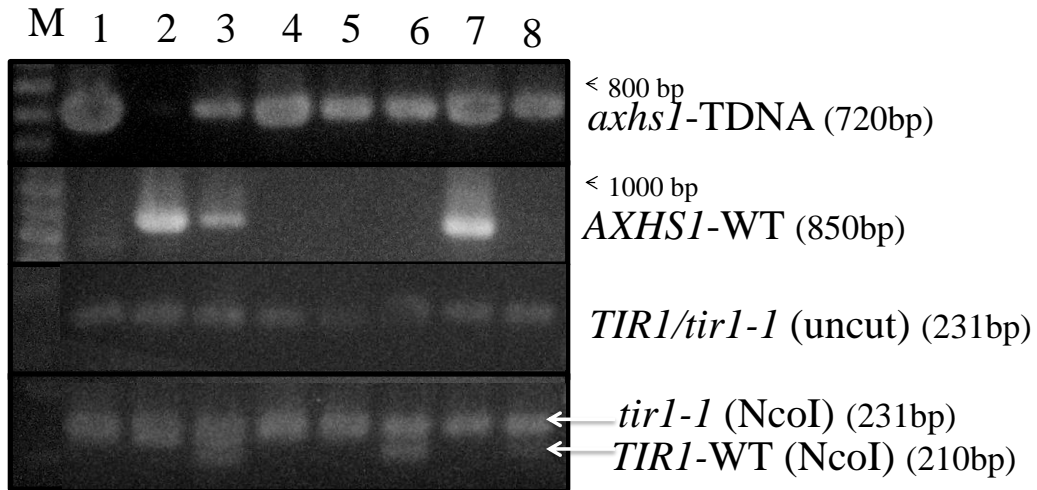

Figure 16. Construction of the *axhs1/dwf4 tir1-1* double mutant. Genomic DNA from F2 progeny of the cross between homozygous *axhs1/dwf4* and *tir1-1* was isolated, and analyzed by PCR as described in Materials and Methods. 1) homozygous *axhs1/dwf4* homozygous *tir1-1,* 2) wild type *AHS1/DWF4* homozygous *tir1-1,* 3) heterozygous *axhs1/dwf4* heterozygous *tir1-1,* 4) homozygous *axhs1/dwf4* homozygous *tir1-1,* 5) homozygous *axhs1/dwf4* homozygous *tir1-1,* 6) homozygous *axhs1/dwf4* heterozygous *tir1-1,* 7) heterozygous *axhs1/dwf4* homozygous *tir1-1,* 8) homozygous *axhs1/dwf4* heterozygous *tir1-1.*

As illustrated in Figure 15, *tir1-1* exhibited resistance to IAA, 2,4-D, NPA, and PCIB in roots. The *axhs1/dwf4 tir1-1* double mutant had an intermediate sensitivity to IAA, 2,4-D, NPA, and PCIB between *axhs1/dwf4* and *tir1-1* (Figure 15). *axhs1/dwf4 tir1-1* appeared very similar to *axhs1/dwf4* plants at seedlings and adult stage (Figure 12). Taken together, these results strongly suggest that *AXHS1/DWF4* functions at the level or downstream of *TIR1*.

The *axhs1/dwf4 axr2-1* double mutant was constructed by genetic crosses between *axhs1/dwf4* and *axr2-1* mutants. The F2 progeny of the cross was analyzed by PCR (Figure 17) as described in Materials and Methods.
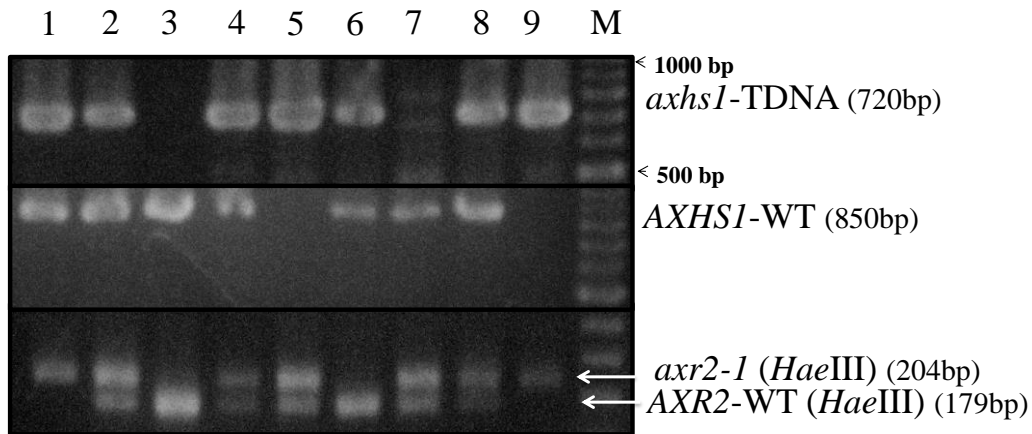

Figure 17. Construction of the *axhs1/dwf4 axr2-1* double mutant. Genomic DNA from F2 progeny of the cross between homozygous *axhs1/dwf4* and *axr2-1* was isolated, and analyzed by PCR as described in Materials and Methods. 1) heterozygous *axhs1/dwf4* homozygous *axr2-1,* 2) heterozygous *axhs1/dwf4* heterozygous *axr2-1,* 3) wild type *AXHS1/DWF4* wild type *AXR2,* 4) heterozygous *axhs1/dwf4* heterozygous *axr2-1,* 5) homozygous *axhs1/dwf4* heterozygous *axr2-1,* 6) heterozygous *axhs1/dwf4* wild type *AXR2,* 7) wild type *AXHS1/DWF4* heterozygous *axr2-1,* 8) heterozygous *axhs1/dwf4* heterozygous *axr2-1,* 9) homozygous *axhs1/dwf4* homozygous *axr2-1.*

Our results indicate that *axr2-1* has increased resistance to PCIB, and a level of sensitivity to NPA similar to that of wild type roots (Figure 15). The *axhs1/dwf4 axr2-1* mutant root growth exhibited levels of sensitivity to IAA, 2,4-D, PCIB, and NPA inhibition similar to those of the *axr2-1* mutant (Figure 15). On the other hand, *axhs1/dwf4 axr2-1* appeared very similar to *axr2-1* plants at both seedling and adult stages (Figure 12). These results indicate that *AXHS1/DWF4* acts upstream of *AXR2 (AUX/IAA7)* in the auxin signaling pathway.

29

We constructed an *axhs1/dwf4 aux1.7* double mutant by genetic crosses. *axhs1/dwf4* and *aux1-7* mutants were crossed, and F2 progeny analyzed by PCR (Figure 18) as described in Materials and Methods.
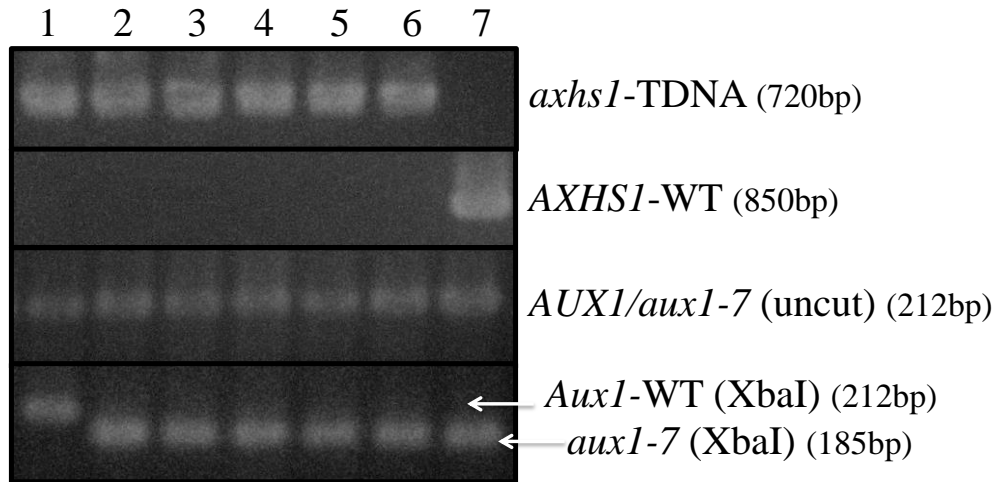

Figure 18. Construction of the *axhs1/dwf4 aux1-7* double mutant. Genomic DNA from F2 progeny of the cross between homozygous *axhs1/dwf4* and *aux1-7* was isolated, and analyzed by PCR as described in Materials and Methods. 1) homozygous *axhs1/dwf4* wild type *AUX1,* 2-6) homozygous *axhs1/dwf4* homozygous *aux1-7,* 7) wild type *AHS1/DWF4* homozygous *aux1-7.*

The *axhs1/dwf4 aux1-7* double mutant had intermediate sensitivity to IAA and 2,4-D between *axhs1* and *aux1-7* (Figure 19). In contrast, the level of sensitivity to NPA and PCIB in *axhs1/dwf4 aux1-7* was very similar to that of the *axhs1/dwf4* mutant (Figure 19). These results indicate that AUX1 mediates IAA and 2,4-D hypersensitivity, but has no significant impact on NPA and PCIB hypersensitivity in *axhs1/dwf4*.
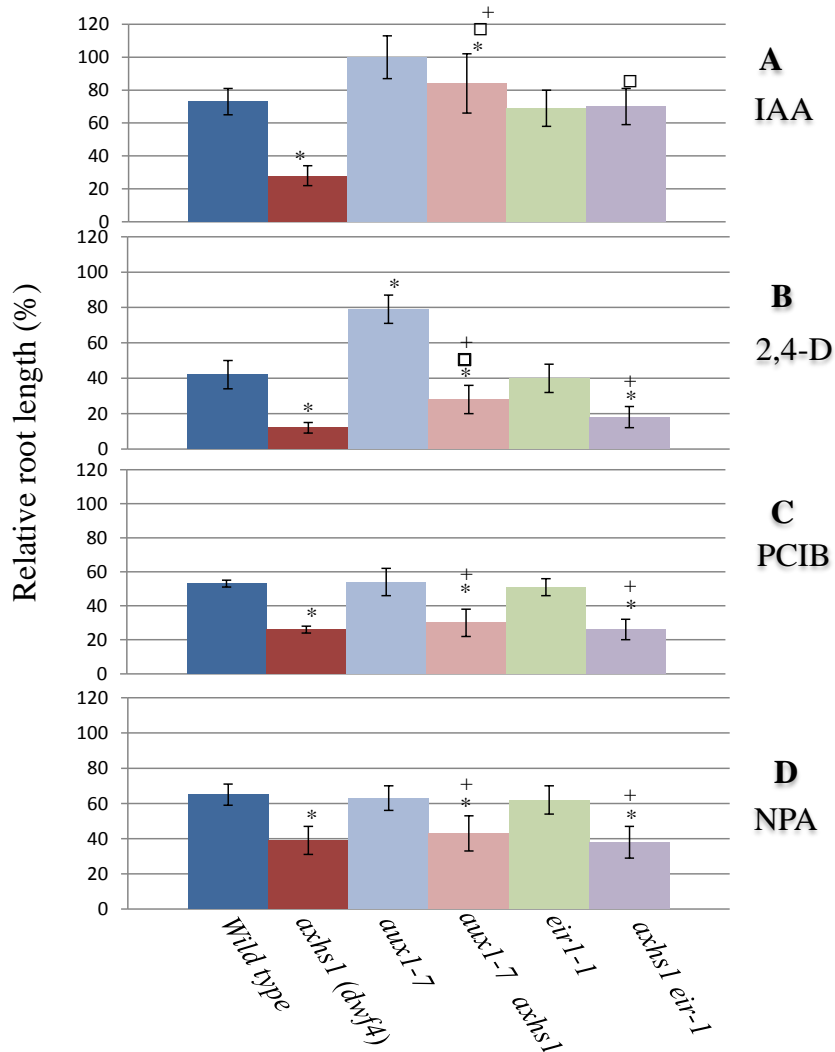
Figure 19. Interaction between *AXHS1/DWF4* and genes involved in auxin transport. Wild type, *axhs1(dwf4)*, *aux1-7*, *axhs1(dwf4) aux1-7*, *eir1-1*, and *axhs1(dwf4) eir1-1* seedlings were grown for 7 days in control medium and 60 nM IAA, 60 nM 2,4-D, 10 μ M PCIB, or 2.5 μ M NPA containing medium. Relative root length is expressed as a percentage of the length observed in unsupplemented medium. Data represent mean $\pm$ SD of more than 20 seedlings from at least two independent experiments. * = significant difference from wild type by Student's t-test ($p<0.05$). □= significant difference from *axhs1/dwf4* by Student's t-test ($p<0.05$). + = significant difference from *aux1-7*, or *eir1-1* by Student's t-test ($p<0.05$).

The root growth of *axhs1/dwf4 aux1-7* seedlings was similar to that of *aux1-7*, but they exhibited a short hypocotyl similar to that of *axhs1/dwf4* (Figure 12A). The morphology of mature *axhs1/dwf4 aux1-7* plants was very similar to that of the *axhs1/dwf4* single mutant (Figure 12B).

The *axhs1/dwf4 eir1-1* double mutant was constructed by genetic crosses between *axhs1/dwf4* and *eir1-1* mutants. The F2 progeny of the cross was analyzed by PCR (Figure 20) as described in Materials and Methods.
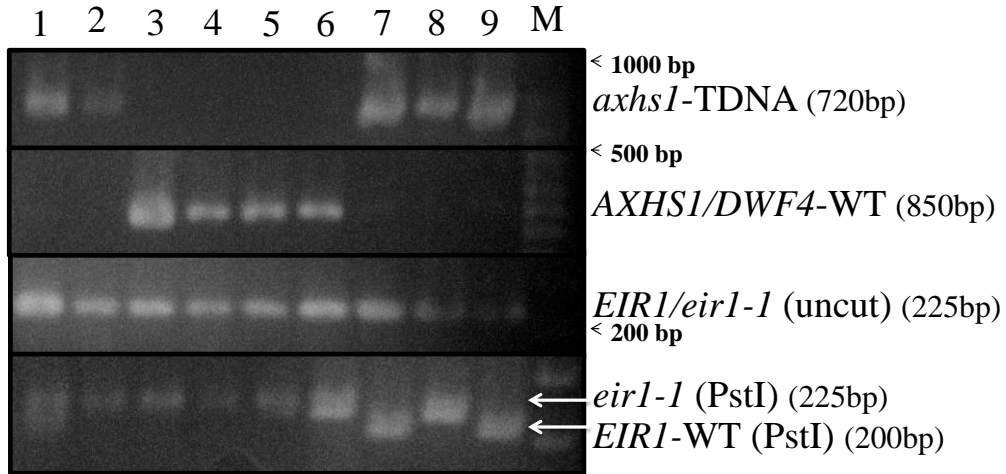

Figure 20. Construction of the *axhs1/dwf4 eir1-1* double mutant. Genomic DNA from F2 progeny of the cross between homozygous *axhs1/dwf4* and *eir1-1* was isolated, and analyzed by PCR as described in Materials and Methods. 1) homozygous *axhs1/dwf4* heterozygous *eir1-1,* 2) homozygous *axhs1/dwf4* homozygous *eir1-1,* 3) wild type *AXHS1/DWF4* homozygous *eir1-1,* 4) wild type *AXHS1/DWF4* homozygous *eir1-1,* 5) wild type *AXHS1/DWF4* homozygous *eir1-1,* 6) wild type *AXHS1/DWF4* homozygous *eir1-1,* 7) homozygous *axhs1/dwf4* wild type *EIR1,* 8) homozygous *axhs1/dwf4* homozygous *eir1-1,* 9) homozygous *axhs1/dwf4* wild type *EIR1.*

The *axhs1/dwf4 eir1-1* double mutant exhibited levels of sensitivity to 2,4-D, NPA and PCIB similar to those of the *axhs1/dwf4* single mutant (Figure 19). In contrast, it displayed wild type sensitivities to IAA (Figure 19). These results indicate that PIN2/EIR1 mediates *axhs1* hypersensitivity to IAA, but has no significant impact on the 2,4-D, NPA and PCIB sensitivity of the mutant. On the other hand, *axhs1/dwf4 eir1-1* seedlings exhibited a short hypocotyl similar to that of *axhs1,* and a root growth similar to that of *eir1-1* (Figure 12A). The morphology of *axhs1 eir1-1* plants at adult stage was indistinguishable from that of the *axhs1/dwf4* mutant (Figure 12B).

In order to further evaluate the impact of the *axhs1/dwf4* mutation on auxin transport, the expression of *AUX1* and *PIN2/EIR1* in the *axhs1/dwf4* mutant was analyzed by RT-PCR analysis. The *PIN2/EIR1* mRNA accumulation level was somewhat lower in *axhs1/dwf4* than in wild type seedlings (Figure 21). In contrast, no significant differences were observed in the expression of *AUX1* between *axhs1/dwf4* and wild type seedlings (Figure 21).
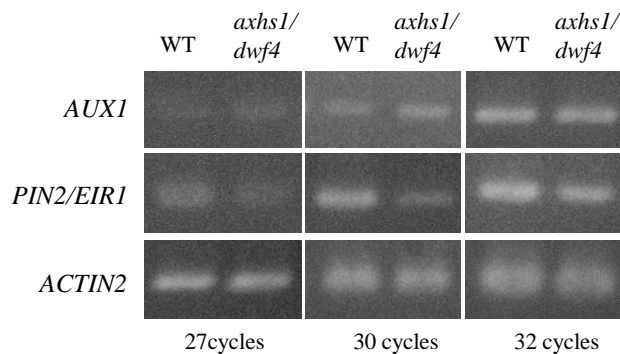

Figure 21. RT-PCR analysis. Seven-day-old wild type and *axhs1/dwf4* seedlings were analyzed for expression of *AUX1* and *PIN2/EIR1*. The number of PCR cycles is indicated. The figure illustrates representative results from three independent experiments.

Auxin sensitivity of BR mutants

In order to further evaluate the cross talk between auxin and BR in controlling root elongation, we examined the growth of mutants affected in BR biosynthesis and BR signaling. *BRI1* encodes a critical component of the BR receptor (Li and Chory 1997; Nam and Li, 2002), and *DWF6/DET2* encodes a putative steroid 5 alpha-reductase that catalyzes an early step of BR biosynthesis (Fujioka et al. 1997) (Figure 8). As shown in Figure 22, *axhs1/dwf4, det2* and *bri1*-6 showed enhanced inhibition of root growth in response to exogenous IAA, 2,4-D, PCIB and NPA. These results indicate that hypersensitivity to auxin and related compounds in roots is regulated by the BR biosynthesis and signal transduction pathways.

33
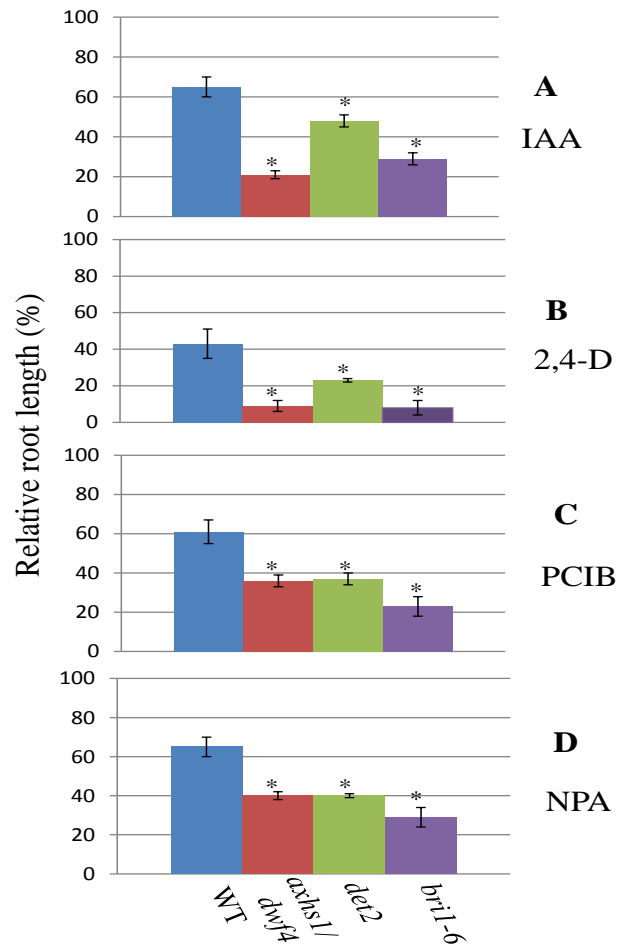
Figure 22. BR biosynthesis and BR signaling mutants are hypersensitive to auxins, antiauxins, and auxin transport inhibitors. Wild type, *axhs1/dwf4, det2*, and *bri1-6* seedlings were grown for 7 days in medium supplemented with or without 60 nM IAA, 60 nM 2,4-D, 10μ M PCIB, or 2.5μ M NPA. Root length is expressed relative to untreated seedlings. Data are means $\pm$ SD (n > 20) from at least two independent experiments. An asterisk indicates a significant difference from wild type by Student's t-test (p<0.05).

Auxin-dependent gene expression in axhs1/dwf4

Our genetic interaction analyses indicate that the AXHS1/DWF4 mediated BR biosynthesis and the auxin signaling pathway cross-talk somewhere downstream of the site of AXR1-TIR1 action and somewhere upstream of the site of AXR2. Next, we analyzed the expression of the auxin-inducible reporter gene *DR5:GUS* in wild type and *axhs1/dwf4* genotypes. The *DR5:GUS* reporter, which contains the AuxRE, is thought to reflect endogenous auxin distribution (Ulmasov et al. 1997). In order to generate

axhs1/dwf4 DR5:GUS plants, we crossed a transgenic line harboring the *DR5:GUS* construct into the *axhs1/dwf4* background. In *axhs1/dwf4* seedlings grown in control medium, the expression of *DR5:GUS* expression was reduced compared to wild type seedlings (Figure 23A). In contrast, *DR5:GUS* and *axhs1/dwf4 DR5:GUS* seedlings treated with BL exhibited similar levels of GUS activity (Figure 23B), which indicates that BR promotes the expression of *DR5:GUS*. On the other hand, *DR5:GUS* expression was increased in wild type and *axhs1/dwf4* seedlings treated with 2,4-D (Figure 23C). The expression of the reporter gene in *axhs1/dwf4* seedlings treated with 2,4-D was reduced in cotyledons, but it was similar to wild type in roots and hypocotyls (Figure 23C). Interestingly, *axhs1/dwf4* seedlings treated with both auxin and BR exhibited higher levels of *DR5:GUS* expression in cotyledons, hypocotyls, and roots compared to those of wild type seedlings (Figure 23D). These results indicate that the cellular balance of auxin and BR concentration may play an important role in the regulation of auxin-responsive genes.
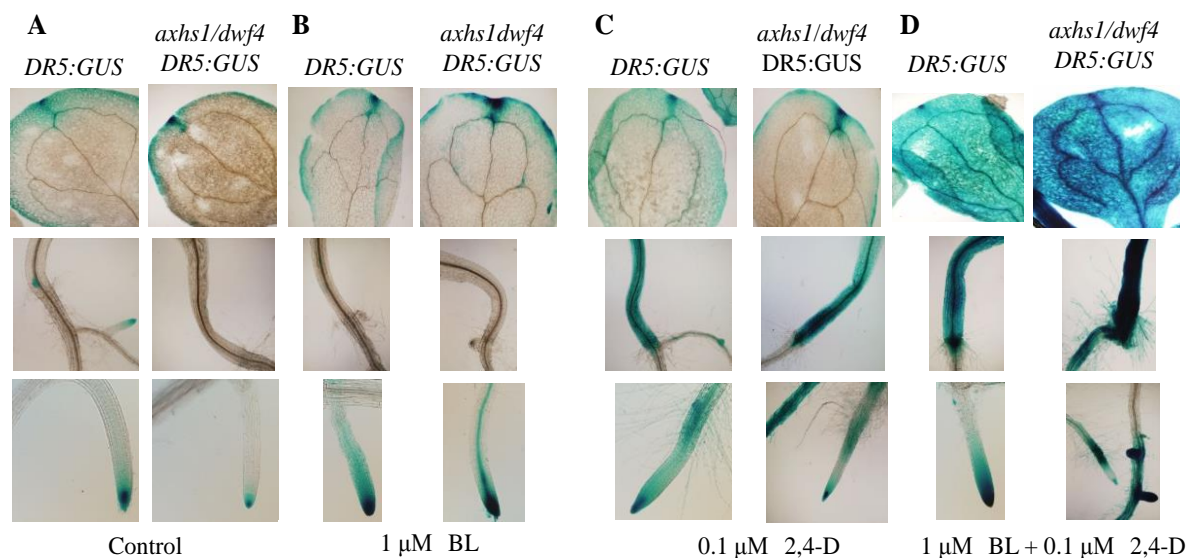
Figure 23. Analysis of the expression of the auxin reporter *DR5:GUS* gene in wild type and *axhs1/dwf4* mutant seedlings. GUS activity was analyzed in *DR5:GUS* and *axhs1/dwf4 DR5:GUS* seedlings grown in agar plates for 7 days and then incubated for 48h in liquid medium (A), and liquid medium supplemented with either 1μ M BL (B), 0.1μ M 2,4-D (C), or 1μ M BL and 0.1μ M 2,4-D (D), respectively. Seedlings were stained for GUS for 20 h, and representative seedlings from three independent experiments were photographed.

Auxin-dependent AUX/IAA protein degradation in axhs1/dwf4

In order to evaluate AUX/IAA protein stability, we used transgenic plants carrying the *HS:AXR3NT-GUS* reporter gene, which encodes a heat shock-inducible fusion of the N-terminal portion of AUX/IAA17(AXR3) and GUS (Gray et al. 2001). We crossed the *HS:AXR3NT-GUS* gene into the *axhs1/dwf4* background and assessed protein stability in *HS:AXR3NT-GUS* and *axhs1/dwf4 HS:AXR3NT-GUS* lines (Figure 24). First, we did time course experiments to determine the level *of* AXR3NT-GUS accumulation in wild type and *axhs1/dwf4* seedlings treated with and without BR (Figure 24A, B). Seedlings of both genotypes were heat shocked for 2 h to promote *AXR3NT-GUS* gene expression, but the stability of the reporter protein in *axhs1* was lower compared to that of wild type (Figure 24A, B). Increased levels of AXR3NT-GUS protein were observed in wild type and *axhs1/dwf4* seedlings treated with BR (Figure 24A, B). Next, we analyzed the effect of auxin and BR interactions on AXR3NT-GUS protein stability (Figure 24C, D). 2,4-D promoted degradation of the reporter protein in wild type and *axhs1/dwf4* seedlings. In contrast, BR prevented AXR3NT-GUS protein degradation in both wild type and *axhs1/dwf4* seedlings treated with and without 2,4-D (Figure 24C, D). These results strongly suggest that BR inhibits auxin mediated degradation of AUX/IAA proteins.
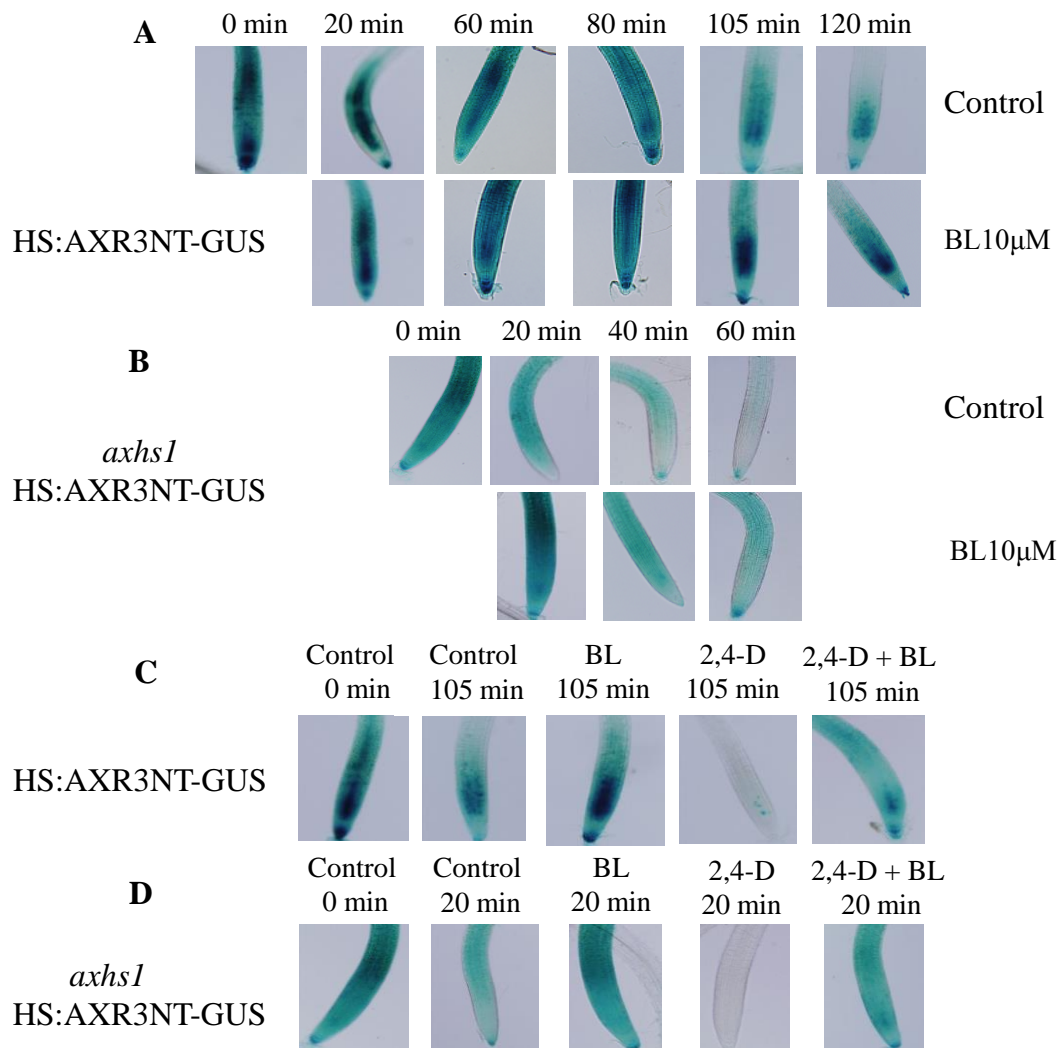
Figure 24. BR prevents the auxin-mediated degradation of an AUX/IAA reporter protein. Seven-day-old *HS:AXR3NT-GUS* (A) and *axhs1/dwf4 HS:AXR3NT-GUS* (B) seedlings were heat shocked at 37°C for 120 min to induce the expression of the fusion protein. After incubation at 23°C for 20 min (time 0), seedlings were transferred to new medium supplemented with or without 10 μ M BL, and incubated for the time periods listed. Seven-day-old *HS:AXR3NT-GUS* (C) and *axhs1/dwf4 HS:AXR3NT-GUS* (D) seedlings were treated as in (A, B) to induce the expression of the reporter protein. After incubation at 23°C for 20 min, seedlings were mock-treated or treated with 10 μ M BL, 5 μ M 2,4-D, and 10 μ M BL and 5 μ M 2,4-D for the indicated periods of time. Seedlings were stained for 20 h to detect GUS activity. The figure illustrates representative results from three independent experiments.

Discussion

Isolation and characterization of the *axhs1* auxin-hypersensitive mutant indicate the involvement of BR in auxin regulated root elongation. Results from BR-feeding experiments, TAIL-PCR, *DWF4* gene expression, and *dwf4* genetic complementation analyses indicated that *axhs1* is a leaky mutation of *DWF4* (Figure 7 and Figure 9). DWF4 is a C-22-α-hydrolase that catalyzes the rate limiting step of BR biosynthesis (Choe et al. 1998). Null *dwf4* mutations (Azpiroz et al. 1998; Nakamoto et al. 2006) are infertile and showed a stronger dwarf phenotype compared to that of *axhs1*, indicating that *axhs1* is a weak allele of *DWF4*.

Nakamoto et al. (2006) found that inhibition of BR biosynthesis by either a leaky mutation of *DWF4* or Brz rescues defects in tropic responses of hypocotyls in the *Arabidopsis nph4*(*arf7*) mutant. In the present study, we show that the *axhs1/dwf4* mutant is hypersensitive to auxins (IAA, 2,4-D), polar auxin transport inhibitors (TIBA, NPA), and inhibitors of the auxin-mediated degradation of AUX/IAA repressor proteins, such as PCIB. These phenotypes can be explained by a mutation affecting auxin biosynthesis, transport, or signaling pathway. Nakamura et al. (2003a) reported that the BR-deficient *det2* mutant exhibited higher IAA levels compared to wild type plants, however, no change in the endogenous IAA levels per gram fresh weight was found following BR treatment of either wild type or *det2* seedlings. In order to evaluate the impact of the *axhs1/dwf4* mutation on auxin biosynthesis, we constructed and characterized a mutant deficient in both auxin and BR biosynthesis. *ASA1* encodes the α-subunit of anthranilate synthase, a rate limiting enzyme of tryptophan biosynthesis (Stepanova et al. 2005). The *wei2-1* mutation had no significant impact on the *axhs1/dwf4* phenotypes (Figure 11 and Figure 12). Taking into account that *wei2-1* suppress the high-auxin phenotypes of *sur1* and *sur2*, two-auxin overproducing mutants (Stepanova et al. 2005), our results strongly suggest that the *axhs1* phenotypes are not caused by an increased amount of auxin in *axhs1/ dwf4*. On the other hand, BR does not affect the expression of a *ASA1:GUS* reporter gene introduced into both *axhs1/dwf4* and

wild type genotypes (Figure 13), which suggests that BR does not have a significant role in regulating the ASA1-mediated auxin biosynthesis pathway.

Since auxin polar transport inhibitors such as NPA and TIBA have been proposed to affect root growth by increasing auxin levels in the root tip, hypersensitivity could result from a change in auxin transport or an increased auxin response in the *axhs1/dwf4* mutant. Thus, mutants such as *tir3* where resistant to NPA and had clear defects in auxin transport (Ruegger et al. 1997), and mutants such as *tir1* were defective in auxin response (Ruegger et al. 2012). Our pharmacological and genetic analyses indicate that AXHS1/DWF4 is involved in both auxin signaling and auxin uptake. The *axhs1/dwf4 eir1-1* double mutant had a level of sensitivity to 2,4-D similar to that of the *axhs1/dwf4* single mutant, whereas it displayed a root growth on IAA similar to that of wild type seedlings (Figure 19). Because IAA and NAA are preferentially transported out of the cells by auxin efflux carriers such as PIN2/EIR1, while 2,4-D largely diffuses (Luschnig et al. 1998, Delbarre et al. 1996), our results indicate that a reduction of the PIN2/EIR1 mediated auxin transport rescues the IAA-hypersensitive phenotype in *axhs1/dwf4*. RT-PCR analysis indicated that the expression of *PIN2/EIR1* is somewhat reduced in *axhs1/dwf4* compared to wild type seedlings (Figure 21), which suggests that BR deficiency caused by *axhs1/dwf4* leads to reduction of PIN2/EIR1-mediated polar auxin transport. Consistent with the above-indicated results, it has been shown that BRs interact with auxin to promote lateral root development and stimulate plant tropisms in roots and hypocotyls through activation of polar transport of auxin in root and shoot (Bao et al. 2004, Li et al. 2005). Li et al. (2005) reported that the expression of *PIN1* and *PIN2/EIR1* genes was induced in wild type plants by BR treatment, whereas it was suppressed in BR biosynthesis-deficient mutants such as *det2/dwf6* and *dim1/dwf1*. In addition, BR induced the basipetal accumulation of PIN2/EIR1 and stimulated the extended localization of the protein into the root elongation zone in response to gravity (Li et al. 2005). Taking into account that AUX1 is not expressed in root cortical cells (Swarup et al. 2001, Swarup et al. 2004), there is the possibility that defects in PIN2/EIR1 protein localization in root epidermal and cortical cells will result in an

altered distribution of auxin between cells of the meristem and root elongation zones in *axhs1/dwf4*.

aux1 mutations disrupt IAA and 2,4-D, but not NAA accumulation (Marchant et al. 1999; Rahman et al. 2001; Swarup et al. 2004). The *axhs1/dwf4 aux1-7* double mutant had an intermediate sensitivity to 2,4-D and IAA between *axhs1/dwf4* and *aux1-7* (Figure 19). In contrast, *axhs1/dwf4, aux1-7,* and *axhs1/dwf4 aux1.7* mutants exhibited wild type levels of sensitivity to the lipophilic synthetic auxin NAA (Figure 6, data not shown). These results indicate that the IAA and 2,4-D hypersensitivity of *axhs1/dwf4* is mediated by an AUX1 dependent auxin uptake, and suggest that auxin influx is accelerated leading to the increase of local concentrations of auxin in the *axhs1/dwf4* mutant. RT-PCR analysis indicated that the level of expression of *AUX1* was similar in wild type and *axhs1/dwf4* seedlings (Figure 21), however, defects in AUX1 protein localization might account for an increased auxin influx in *axhs1/dwf4*.

Nakamura et al. (2006) reported that AUX/IAA proteins may function as signaling components modulating auxin and BR responses in an organ-dependent manner (Nakamura et al. 2006). Our results indicate that mutants affected in auxin signal transduction (*axr1.3, axr2.1, tir1.1*) were resistant to the antiauxin PCIB, while those affected in auxin transport (*aux1-7, eir1-1*) exhibited wild type sensitivity to that antiauxin (Figure 15 and Figure 19). Thus, auxin and PCIB hypersensitivity could be explained by an increased auxin response in the *axhs1/dwf4* mutant. *det2* and *bri1-6* mutants were also hypersensitive to auxins and the antiauxin PCIB (Figure 22), which suggests that homeostatic control of BR signaling is required for a normal response to auxin. On the other hand, genetic interaction analyses indicate that AXHS1/DWF4 and the auxin signaling pathway cross-talk somewhere downstream of the site of AXR1-TIR1 action and somewhere upstream of the site of AXR2 (AUX/IAA7) action (Figure 12, and Figure 15). Moreover, the results of our *AXR3NT-GUS* protein stability assays strongly suggest that BR prevents the auxin-dependent degradation of the AUX/IAA17 (AXR3) protein through the ubiquitin-proteasome pathway (Figure 24). Nemhauser et al. (2004) reported that treatment with 1μ M BR does not induce

AXR3NT-GUS protein turnover in wild type seedlings. They did time course experiments, but they did not do extensive quantification of the later time points (80 and 150 min after the end of the heat shock period), where, judging from the published images, increased stability of the reporter would be detected (J. Nemhauser, personal communication). We did time course experiments to analyze the effects of 10μ M BR on AXR3NT-GUS protein degradation in wild type and *axhs1/dwf4* roots (Figure 24A, B). After that, we focused on BR concentration: a) wild type BR levels, b) reduced BR levels (*axhs1/dwf4* seedlings), c) increased BR levels (treatment with 10μ M BR). Our results indicate that BR prevents AXR3NT-GUS protein degradation in both wild type and *axhs1* mutant seedlings treated with and without 5μ M 2,4-D (Figure 24C, D).

DR5:GUS expression analyses (Figure 23) indicate that the expression of *DR5:GUS* was reduced in the *axhs1/dwf4* mutant, but rescued by BR administration, suggesting that BRs are essential for full induction of the reporter gene. BR-treated seedlings showed higher levels of and broader *DR5:GUS* expression from the root tip to the elongation zone (Figure 23A, B). Besides, GUS expression in *axhs1/dwf4* seedlings treated with exogenous auxin was reduced in cotyledons, but it was similar to wild type in roots and hypocotyls (Figure 23C). Since the *axhs1/dwf4* mutation inhibits the actions of exogenously applied auxin, results indicate that AXHS1/DWF4 may function downstream of auxin and somewhere upstream of *DR5:GUS*. Interestingly, *axhs1/dwf4* seedlings treated with both auxin and BR exhibited higher levels of *DR5:GUS* expression in cotyledons, hypocotyls, and roots compared to those of wild type seedlings (Figure 23D).

Results from our pharmacological, genetic interaction, *DR5:GUS* expression, and AXR3NT-GUS protein degradation analyses can be explained by a BR-deficiency activation of auxin signaling, but not just by an accelerated auxin influx leading to the increase of intracellular auxin in root apical tissues of *axhs1/dwf4*. Collectively, the data indicate that is not the absolute level of auxin and BR concentration, but the concentration ratio that may play an essential role in the regulation of auxin and BR mediated responses, such as root elongation.

The BRI1 plasma membrane localized receptor serine/threonine kinase is essential for BR perception. When BR levels are low, the cytoplasmic BIN2 kinase phosphorylates and inactivates transcription factors such as BZR1 and BES1, which results in their cytoplasmic accumulation and proteasome mediated degradation. Upon BR perception, BIN2 is inactivated, which allows hypophosphorylated BESI/BZR1 proteins to accumulate in the nucleus, where they trigger the BR response (Gruszka 2013).

The expression of *DWF4* either decreased or increased in response to exogenously applied BL and Brz, respectively (Yoshimitsu et al. 2011). On the other hand, auxin stimulates *DWF4* expression and BRs biosynthesis through the auxin-signaling pathway (Chung et al. 2011, Yoshimitsu et al. 2011). Here, we propose a model of interaction between BR and auxin which is focused on the importance of the ratio of the endogenous auxin-to-BR concentration as an essential factor for modulating auxin transport and the stability of at least part of the members of the AUX/IAA protein family (Figure 25). According to our model, BR-deficiency promotes AUX/IAA protein degradation by both a modification of auxin transport leading to an altered auxin distribution between cells of the meristem and root elongation zone, and a direct activation of auxin signaling somewhere downstream of the site of AXR1-TIR1 action and somewhere upstream of the site of AXR2 (AUX/IAA7) action. Increased BR level prevents the auxin-mediated degradation of AUX/IAA proteins, and subsequently inhibits the auxin signaling pathway, including the DWF4-mediated BR biosynthesis (Figure 25). The complex biological significance of this model of interaction between auxin and BR should be determined in further studies.
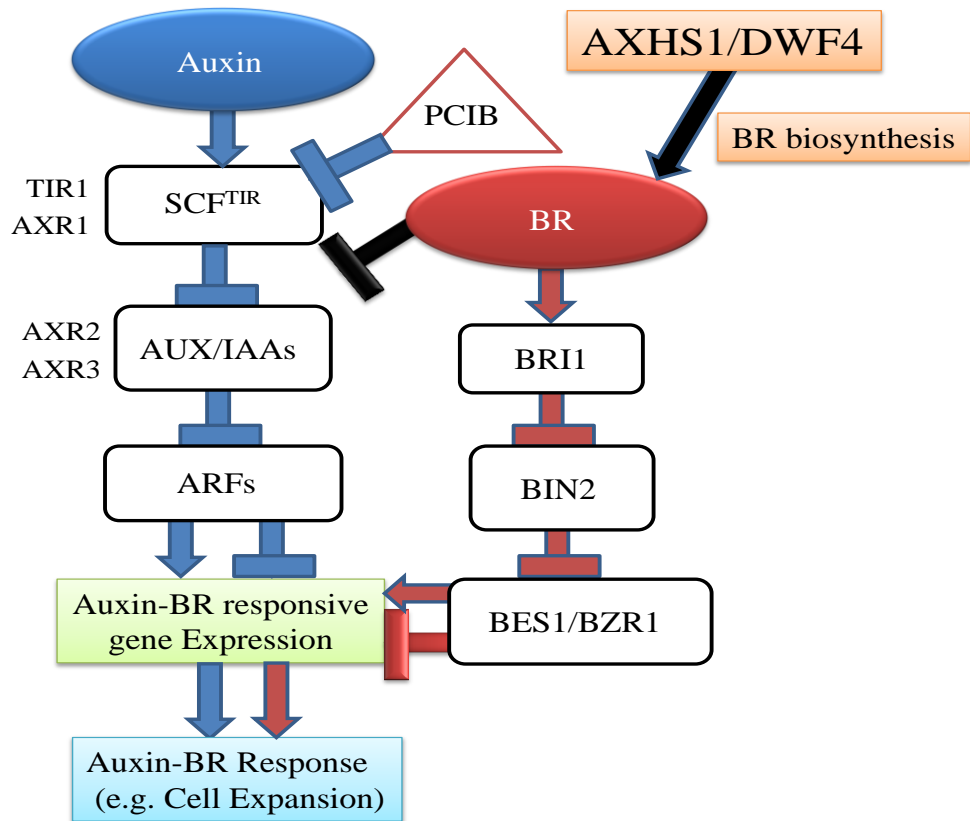
Figure 25. Model of interaction between brassinosteroid and auxin signaling pathways.

ARFs, auxin response factors; AUX/IAAs, repressor proteins; BES1/BZR1, transcription factors; BIN2, protein kinase; BRI1, BR receptor; SCF^{TIR1}, serine/threonine kinase-cullin-F-box protein complex; TIR1, auxin receptor.

References

Alonso JM, Stepanova AN, Leisse TJ, Kim CJ, Chen H, Shinn P, Stevenson D K, Zimmerman J, Barajas P, Cheuk R, Gadrinab C, Heller C, Jeske A, Koesema E, Meyers CC, Parker H, Prednis L, Ansari Y, Choy N, Deen H, Geralt M, Hazari N, Hom E, Karnes M, Mulholland C, Ndubaku R, Schmidt I, Guzman P, Aguilar-Henonin L, Schmid M, Weigel D, Carter DE, Marchand T, Risseeuw E, Brogden D, Zeko A, Crosby WL, Berry CC, Ecker JR (2003) Genome-wide insertional mutagenesis of *Arabidopsis thaliana.* Science 301: 653-657.

Azpiroz R, Wu Y, LoCascio JC, Feldman KA (1998) An *Arabidopsis* brassinosteroid-dependent mutant is blocked in cell elongation. *Plant Cell* 10:219-230.

Bao F, Shen J, Brady SR, Muday GK, Asami T, Yang Z (2004) Brassinosteroid interact with auxin to promote lateral root development in *Arabidopsis*. *Plant Physiol* 134:1624-1631.

Choe S, Dilkes BP, Fujioka S, Takatsuto S, Sakurai A, Feldman KA (1998) The *DWF4* gene of *Arabidopsis* encodes a Cytochrome P450 that mediates multiple 22α-Hydroxylation steps in brassinosteroid biosynthesis. *Plant Cell* 10:231-243.

Chung Y, Maharjan PM, Lee O, Fujioka S, Jang S, Kim B, Takatsuto S, Tsujimoto M, Kim H, Cho S, Park T, Cho H, Hwang I,Choe S. (2011) Auxin stimulates *DWARF4* expression and brassinosteriod biosynthesis in *Arabidopsis*. *Plant J* 66:564-578.

Delbarre A, Muller P, Imhoff V, Guern J (1996) Comparison of mechanisms controlling uptake and accumulation of 2,4-dichloro-phenoxy acetic acid, naphthalene-1-acetic acid, and indole-3-acetic acid in suspension-cultured tobacco cells. *Planta* 198:532-541.

Fujioka S, Li J, Choi YH, Seto H, Takatsuto S, Noguchi T et al. (1997) The *Arabidopsis* deetiolated2 mutant is blocked early in brassinosteroid biosynthesis. *Plant Cell* 9:1951-1962.

Goda H, Sawa S, Asami T, Fujioka S, Shimada Y, Yoshida S (2004) Comprehensive comparison of auxin-regulated and brassinosteroid-regulated genes in *Arabidopsis*. *Plant Physiol* 134:1555-1573.

Gray WM, Kepinski S, Rouse D, Leyser O, Estelle M (2001) Auxin regulates SCFTIR1-dependent degradation of AUX/IAA proteins. *Nature* 414:271-276.

Gruszka D (2013) The brassinosteroid signaling pathway, new key players and interconnections with other signaling networks crucial for plant development and stress tolerance. *Int J Mol Sci* 14:8740-8774.

Haughn GW, Somerville C (1986) Sulfonylurea-resistant mutants of *Arabidopsis thaliana*. *Mol Gen Genet* 204:430-434.

Hayashi KI, Jones AM, Ogino K, Yamazoe A, Oono Y, Inouchi M, Kondo H, Nozaki H (2003) Yokonolide B, a novel inhibitor of auxin action, blocks degradation of AUX/IAA factors. *J Biol Chem* 278:23797-23806.

Lau S, Jurgens G, De Sme ID (2008) The evolving complexity of the auxin pathway. *Plant Cell* 20:1738-1746.

Leyser HM, Lincoln CA, Timpte C, Lammer D, Turner J, Estelle M (1993) *Arabidopsis* auxin-resistance gene AXR1 encodes a protein related to ubiquitin-activating enzyme E1. *Nature* 364:161-164.

Li J, Chory J (1997) A putative leucine-rich repeat receptor kinase involved in brassinosteroid signal transduction. *Cell* 90:929-938.

Li L, Xu J, Xu ZH, Xue HW (2005) Brassinosteroid stimulate plant tropisms thorough modulation of polar auxin transport in *Brassica* and *Arabidopsis*. *Plant Cell* 17:2738-2753.

Liu YG, Mitsukawa N, Oosumi T (1995) Efficient isolation and mapping of *Arabidopsis thaliana* T-DNA insert junctions by thermal asymmetric interlaced PCR. *Plant J* 8:457-462.

Luschnig C, Gaxiola RA, Grisafi P, Fink GR (1998) EIR1, a root-specific protein involved in auxin transport, is required for gravitropism in *Arabidopsis thaliana*. *Genes Dev* 12:2175-2187.

Mashiguchi K, Tanaka K, Sakai T, Sugawara S, Kawaide H, Natsume M, Hanada A, Yaeno T, Shirasu K, Yao H, McSteen P,Zhao Y, Hayashi K, Kamiya Y, Kasahara H (2011) The main auxin biosynthesis pathway in *Arabidopsis*. *Proc Natl Acad Sci USA* 108:18512-18517.

Marchant A, Kargul J, May ST, Muller P, Delbarre A, Perrot-Rechenmann C, Bennet MJ (1999) AUX1 regulates root gravitropism in *Arabidopsis* by facilitating auxin uptake within root apical tissues. *EMBO J* 18:2066-2073.

Marchant A, Bhalerao R, Casimiro I, Eklof J, Casero PJ, Bennet MJ, Sandberg G (2002) AUX1 promotes lateral root formation by facilitating indole-3-acetic-acid distribution between sink and source tissues in the *Arabidopsis* seedling. *Plant Cell* 14:589-597.

Muller A, Guan C, Galweiler L, Tanzler P, Huijser P, Marchant A, Parry G, Bennett M, Wisman E, Palme K (1998) *AtPIN2* defines a locus of *Arabidopsis* for root gravitropism control. *EMBO J* 17:6903-6911.

Nagpal P, Walker LM, Young JC, Sonawala A, Timpte C, Estelle M, Reed JW (2000) *AXR2* encodes a member of the AUX/IAA protein family. *Plant Physiol* 123:563-573.

Nakamoto D, Ikeura A, Asami T, Yamamoto K (2006) Inhibition of brassinosteroid biosynthesis by either a *dwarf4* mutation or a brassinosteroid biosynthesis inhibitor rescues defects in tropic responses of hypocotyls in the *Arabidopsis* mutant *nonphototropic hypocotyl 4*. *Plant Physiol* 141:456:464.

Nakamura A, Higuchi K, Goda H, Fujiwara MT, Sawa S, Koshiba T, Shimada Y, Yoshida S (2003a) Brassinolide induces IAA5, IAA19, and DR5, a synthetic auxin response element in *Arabidopsis,* implying a cross talk point of brassinosteroid and auxin signaling. *Plant Physiol* 133: 1843-1853.

Nakamura A, Shimada Y, Goda H, Fujiwara MT, Asami T, Yoshida S (2003b) AXR1 is involved in BR-mediated elongation and *SAUR-AC1* gene expression in *Arabidopsis*. *FEBS Lett* 553:28-32.

Nakamura A, Nakajima N, Goda H, Shimada Y, Hayashi K, Nozaki H, Asami T, Yoshida S, Fujioka S (2006) *Arabidopsis* AUX/IAA genes are involved in brassinosteroid-mediated growth responses in a manner dependent on organ type.

Plant J 45:193:205.

Nam KH, Li J. (2002) BRI1/BAK1, a receptor kinase pair mediating brassinosteroid signaling. *Cell* 102:203-12.

Nemhauser JL, Mokler TC, Chory J (2004) Interdependency of brassinosteroid and auxin signaling in *Arabidopsis*. *PlosS Bio* 2:E258.

Oono Y, Ooura C, Rahman A, Aspuria ET, Hayashi K, Tanaka A, Uchimiya H (2003) *p*-chlorophenoxyisobutiric acid impairs auxin response in *Arabidopsis* root. *Plant Physiol* 133:1135-1147.

Rahman A, Ahamed A, Amakawa T, Goto N, Tsurumi S (2001) Chromasaponin I specifically interacts with AUX1 protein in regulating the gravitropic response of *Arabidopsis* roots. *Plant Physiol* 125:990-1000.

Rahman A, Bannigan A, Sulaman W, Pechter P, Blancaflor EB, Baskin TI (2007) Auxin, actin and growth of the *Arabidopsis thaliana* primary root. *Plant J* 50: 514–528.

Rahman A, Takahashi M, Shibasaki K, Wu S, Inaba T, Tsurumi S, Baskin TI (2010) Gravitropism of *Arabidopsis thaliana* roots requires the polarization of PIN2 toward the root tip in meristematic cortical cells. *Plant Cell* 22:1762-1776.

Ruegger M, Dewey E, Hobbie L, Brown D, Benasconi P, Turner J, Muday G, Estelle M (1997) Reduced NPA-binding in the *tir3* mutant of *Arabidopsis* is associated with a reduction of polar auxin transport and diverse morphological defects. *Plant Cell* 9:745-757.

Ruegger M, Dewey E, Gray WM, Hobbie L, Turner J, Estelle M (2012) The TIR1 protein of *Arabidopsis* functions in auxin response and is related to human SKP2 and yeast Grr1p. *Genes Dev* 12:198-207.

Stepanova AN, Hoyt JM, Hamilton AA, Alonso JM (2005) A link between ethylene and auxin uncovered by the characterization of two root-specific ethylene-insensitive mutants in *Arabidopsis*. *Plant Cell* 17:2230-2242.

Swarup R, Friml J, Marchant A, Ljung K, Sandberg G, Palme K, Bennet M (2001) Localization of the auxin permease AUX1 suggests two functionally distinct hormone

transport pathways operate in the *Arabidopsis* root apex. *Genes and Dev* 15:2648-2653.

Swarup R, Kargul J, Marchant A, Zadik D, Rahman A, Mils R, Yemm A, May S, Williams L, Millner P, Tsurumi S, Moore I, Napler R, Kerr ID, Bennett MJ (2004) Structure-function analysis of the presumptive *Arabidopsis* auxin permease AUX1. *Plant Cell* 16:3069-3083.

Ulmasov T, Murfett J, Hagen G, Guilfoyle TJ (1997) AUX/IAA proteins repress expression of reporter genes containing natural and highly active synthetic auxin response elements. *Plant Cell* 9:1963-1971.

Yoshimitsu Y, Tanaka K, Fukuda W, Asami T, Yoshida S, Hayashi K, Kamiya Y, Jikumaru Y, Shigeta T, Nakamura Y, Matsuo T, Okamoto S (2011) Transcription of *DWARF4* plays a crucial role in auxin-regulated root elongation in addition to brassinosteroid homeostasis in *Arabidopsis thaliana*. *PlosS Bio* 6:E23851.

Woodward AW, Bartel B (2005) Auxin: regulation, action, and interaction. *Ann Bot London* 95:707-735.

Wu G, Lewis DR, Spalding P (2007) Mutations in *Arabidopsis* multidrug resistance-like ABC transporters separate the roles of acropetal and basipetal auxin transport in lateral root development. *Plant Cell* 19:1826-1837.

Publication

Nagase T, Takase H, Sekiya J. Prieto R (2015) The *axhs1/dwf4* auxin-hypersensitive mutant of *Arabidopsis thaliana* defines a link for integration of auxin and brassinosteroid mediated root elongation. *Plant Biotechnology,* 32(2):125-137.

Acknowledgments

I would like to express my great gratitude to Associate Professor Rafael Prieto, Department of Bioscience and Biotechnology, Faculty of Bioenvironmental Science, Kyoto Gakuen University, for his warm encouragement, support, and guidance throughout the course of this research.

I wish to express my sincere thanks to Professor Jiro Sekiya, Professor Hisabumi Takase, and Professor Susumu Yazawa of the Faculty of Bioenvironmental Science, Kyoto Gakuen University, for their encouragement and useful advices.

I also would like to thank members of the Plant Biotechnology Laboratory for their useful discussion and an enjoyable laboratory life.

Finally, I am very grateful to my parents, Kouji and Hideko, for their continuous encouragement and support.

<div align="right">

July, 2015

Taisuke Nagase

</div>